

Dynamic processes in the ionosphere during magnetic storms from the Kharkov incoherent scatter radar observations

L. F. Chernogor,¹ Ye. I. Grigorenko,² V. N. Lysenko,² and V. I. Taran²

Received 4 July 2005; revised 25 September 2006; accepted 6 July 2007; published 26 October 2007.

[1] Results of studying the ionosphere behavior during several magnetic storms of various intensities are presented. The features of pronounced negative ionospheric disturbances accompanying the severe magnetic storms on 25 September 1998 and 29–30 May 2003 ($Kp \approx 8$) are considered. Among them there are a decrease in the electron density by a factor of 3–4, uplifting of the ionospheric $F2$ layer by 100–160 km, increase in the temperature of the charged and neutral atmospheric components, and infringement of plasma transfer processes and thermal balance in the ionosphere–plasmasphere system. In the morning of 25 September 1998, an unusual increase in the upward plasma drift velocity was registered. On 29–30 May 2003 during the storm main phase, a depletion of the relative density of hydrogen ions by more than an order of magnitude was observed that could manifest an emptying of the magnetic flux tube over Kharkov. These effects are explained in terms of thermospheric disturbances, Joule heating, particle precipitation, penetration of magnetospheric electric fields to midlatitudes, the shift of the main ionospheric trough and related structures toward the radar latitude, etc. The ionospheric storm on 20–21 March 2003 had two phases. Its strong negative phase proceeded against a background of a minor geomagnetic disturbance ($Kp \approx 5$). The destabilizing impact of the electric field pulse and traveling atmospheric disturbance generated by magnetospheric substorms could be the cause of the change in the storm phase that occurred in the sunset period. *INDEX TERMS:*

2431 Ionosphere: Ionosphere/magnetosphere interactions; 2788 Magnetospheric Physics: Magnetic storms and substorms; 6969 Radio Science: Remote sensing; *KEYWORDS:* ionosphere; magnetic storms; incoherent scatter radar observations.

Citation: Chernogor, L. F., Ye. I. Grigorenko, V. N. Lysenko, and V. I. Taran (2007), Dynamic processes in the ionosphere during magnetic storms from the Kharkov incoherent scatter radar observations, *Int. J. Geomagn. Aeron.*, 7, GI3001, doi:10.1029/2005GI000125.

1. Introduction

[2] Ionospheric storms are one of manifestations of space weather disturbances. The disturbances are caused by non-stationary processes on the Sun: solar flares and solar storms accompanied by ejection of coronal mass (CME) and magnetic clouds, enhancement of the dynamical pressure of the solar wind, variations in the parameters of the interplanetary magnetic field (IMF), etc. These disturbances covering the

interplanetary space and the Sun–Earth system influence the processes in various regions of the near-Earth environment. On the Earth, the storms cause malfunctions in operation of powerful energetic systems, navigation and remote radio communication systems, and influence the weather [German and Goldberg, 1981], and possibly the human health and the state of the entire biosphere [Vladimirsky *et al.*, 1995]. A large number of publications has been dedicated to studies of ionospheric disturbances accompanying geomagnetic storms (see, e.g., reviews by Danilov and Morozova [1985], Prölss [1995], and Buonsanto [1999]). The accumulated material demonstrates a variety and complicated interaction of the processes forming storms. The latter fact makes each storm a unique event and due to this it is difficult to forecast the ionospheric disturbances. The peculiarity of ionospheric storms is their global character. They cover the entire ionosphere from high latitudes to the equator. However, the

¹Kharkov V. Karazin National University, Kharkov, Ukraine

²Institute of the Ionosphere, National Academy of Sciences of Ukraine, Ministry of Education and Science of Ukraine, Kharkov, Ukraine

Table 1. Relative RMS Error in Estimating the Ionospheric Parameters at an 15-min Signal Integration

h , km	q_{sn}	δN_e	δT_e	δT_i
450	10.0	0.014	0.008	0.006
700	1.0	0.028	0.01	0.01
800	0.5	0.042	0.015	0.014
930	0.2	0.088	0.04	0.03

manifestation of their development depends on many geophysical factors. The complexity of physical processes and relative contribution of different physical mechanisms at different geographical regions lead to a large variety of the observed phenomena at different locations. The analysis of each storm provides valuable information for further studies in the solar-terrestrial physics and also for forecasting of the ionospheric response in the particular region to disturbances on the Sun.

[3] The goal of this paper is the comparative analysis of the peculiarities in the ionospheric behavior during three geomagnetic storms different by their development character and intensity. The observations have been carried out by the Kharkov incoherent scatter (IS) radar.

2. The Observational Facilities

[4] The sounding of the F region and the topside ionosphere was conducted at a frequency of 158 MHz with the incoherent scatter radar of the Institute of the Ionosphere. The radar is located in the vicinity of Kharkov. The geographic and geomagnetic coordinates are 49.6°N, 36.3°E and 45.7°, 117.8°, respectively. The radar description was presented in a series of papers [see, e.g., *Akimov et al.*, 2002; *Grigorenko et al.*, 2003b; *Taran*, 1979, 2001]. The radar is equipped with a zenith double-reflector parabolic antenna with the diameter of 100 m that is one of the largest in the world. The antenna effective area, gain and half-power beam width are about 3700 m², 12,700 and 1°, respectively. The measurements of ionospheric parameters were conducted by the sounding pulses with the circular polarization, the repetition frequency of 24.4 Hz, and the height resolution of 20 (10) and 120 km in the height ranges 100–550 and 200–1500 km, respectively. The radar has a two-channel structure. The pulse power of the transmitting facility is 2.4–3.6 MW depending on the operation mode. The noise temperatures of the two-channel receiving facility and the system as a whole are 150–240 and 570–1320 K, respectively. The bandwidth of the receiving facility filters is 5.5–9.5 kHz. Output signals from the receiver quadrature channels come to two fast operating programmed two-channel correlators that are connected to the local network of the measuring-computing system of online initial processing of IS signals.

[5] Ionosonde “Basis” operated in the mode of vertical sounding with the pulses of 100 μ s duration and repetition frequency of 50 Hz. The height-frequency characteristics (ionograms) were used to determine the critical frequency

f_oF2 of the $F2$ layer and for a calibration of the electron density profile obtained by the IS technique.

3. Methods of Measurements and Data Processing

[6] The ionosphere investigation by the Kharkov IS radar is based on the measurements of the signal correlation function (CF). Measurement and data processing methods were described by *Taran* [1979, 2001], *Emel'yanov* [1999], *Lysenko* [1999a, 1999b, 2001], and *Pulyaev* [1999]. From the measured CFs, electron T_e and ion T_i temperatures, ion composition, vertical component V_z of the plasma drift velocity and other ionospheric parameters are derived. The electron density profiles $N_e(h)$ are obtained using the power profile method from the following formula [*Evans*, 1969]:

$$N_e(h) = C_r q(h) h^2 \left[1 + \frac{T_e(h)}{T_i(h)} \right] \quad (1)$$

where h is the height of the center of the plasma scattering volume, q is the signal-to-noise ratio, and C_r is the proportionality coefficient determined by technical parameters of the radar. For Kharkov radar absolute values of $N_e(h)$ were determined by normalizing the profile and the adjustment of its maximum to the $N_m F2$ value calculated from the critical frequency f_oF2 measured by the ionosonde.

[7] The errors in estimation of the signal CFs and ionospheric parameters depend on the signal-to-noise ratio, noise background, parameters of the equipment, and other factors. Table 1 shows the statistical errors of ionospheric parameters for typical daytime conditions, 15-min signal integration, and the given signal-to-noise ratios.

[8] The vertical plasma velocity V_z is found from the Doppler shift of the IS signal spectrum estimated based on the measured quadrature components of the signal CF [*Emel'yanov*, 1999]. To increase the accuracy of the measurements, a trapezoidal smoothing of CF over altitude is performed [*Holt et al.*, 1992; *Lysenko*, 1999a]. The RMS deviation σ_{V_z} of the measured velocity depends on the signal-to-noise ratio q and varies with altitude. Usually, $\sigma_{V_z} \approx 5 - 20$ m s⁻¹ for altitudes of the ionospheric F region at $q \geq 0.2$ and an integration time of 15 min.

[9] The method used to determine T_i and T_e temperatures should be considered in more detail. These temperatures are calculated taking into account the ion composition at altitudes below the $F2$ layer peak. In this case the T_e/T_i and T_i/m_i ratios, where m_i is ion mass, are found from the measured CFs of a scattered signal [*Farley*, 1969] by comparing these functions with the theoretical CFs using the least squares technique. Certain conditions are imposed in order to eliminate the ambiguity in the solution of the problem [*Pavlov et al.*, 1999; *Schlesier and Buonsanto*, 1999]. The average molecular weight of ions (O_2^+ and NO^+) was taken equal to 31. Gradual transition from the 100% concentration of molecular ions at 120 km altitude (where it was considered that $T_e \approx T_i \approx T_n \approx 355$ K) to

the 100% concentration of O^+ ions at an altitude of 230–300 km was assumed. This height was selected depending on specific conditions: day–night, winter–summer. A change in T_i within an altitude interval of 10 km is restricted additionally: $\Delta T_i(\text{max}) = \pm 0.1T_i$. It should be noted that the applied technique only approximately reflects changes in the concentration of molecular ions, which are especially significant during magnetic disturbances, and results in additional error in determining T_i , T_e , and N_e . The problem of correcting measured ionospheric parameters T_i , T_e , and N_e depending on the applied model of ion composition was first discussed by *Waldteufel* [1971]. It is known that this problem is solved in the modern models of the ionosphere [see, e.g., *Mikhailov and Schlegel*, 1997; *Schlesier and Buonsanto*, 1999]. A comparison of the data on electron density obtained by the Kharkov radar using the power profile technique and the Faraday rotation measurements (this technique is described, e.g., by *Grigorenko* [1979]) made it possible to estimate the error in determining T_i and T_e below $F2$ region peak. This error was not higher than 15% under quiet conditions.

4. Results of Observations and Modeling: Data Analysis

[10] Traditionally, considerable deviation ($\geq 20\%$) of the $F2$ -layer critical frequencies from the median values over a long period of time (from half a day to 2–3 days) usually accompanying a magnetic storm is called an ionospheric storm. It is known [see, e.g., *Buonsanto*, 1999; *Prölss*, 1995] that the ionospheric and thermospheric effects of a storm are closely coupled. In this section we present a brief description of ionospheric and thermospheric disturbances over Kharkov accompanying three magnetic storms with a different character.

4.1. The magnetic storm on 25 September 1998

[11] The magnetic storm on 25 September 1998 was associated with the M6/3B solar flare that occurred during 0644–1009 UT on 23 September 1998. The parameters of heliogeophysical situation are shown in Figure 1¹ (<http://sec.noaa.gov>, <http://swdcwww.kugi.kyoto-u.ac.jp/index.html>). The first three observation days on 21–23 September 1998 that preceded the storm interval were weakly disturbed days ($A_p = 14, 10, 14$). A storm began on 24 September (maximum index $K_p \approx 5$, $A_p = 28$) (see Figure 1). The disturbance rose to severe magnetic storm on 25 September. The storm was initiated by the arrival of interplanetary shock associated with the M6/3B flare and registered with the ACE satellite about 2300 UT on 24 September. The shock was followed by the southward turning of the

IMF B_z component with a maximum deflection of -18 nT at 2333 UT. The solar wind parameters changed (see Figure 1), the temperature T increased up to about 7×10^5 K and the speed from 440 to 880 km s^{-1} . The dynamic pressure of solar wind reached 10 nPa value and the energy ε , transferred to the magnetosphere comprised 75–100 GJ s^{-1} . The solar flare was accompanied by the ejections of energy particles. A greater than 10 MeV energy proton flux reached its maximal level after the midnight on 25 September. The maximum precipitations of electrons were observed during the main storm phase. The variations in the H_p component of the geomagnetic field were significant on 25 September. Index Dst during the main phase of the storm rapidly decreased to -202 nT value at 0800 UT and stayed at the level about -200 nT until 1100 UT. The Kp index reached a maximum value of 8+ during 0600–0900 UT. The recovery phase began after 1100 UT and continued at least to the end of observation. Against a background of the storm the sequence of the intense substorms with index $AE = 1200 - 2000$ nT was registered at night 24–25 and on 25 September. During the days under consideration, the solar activity was moderate with $F_{10.7} = 139$ on 25 September, and 81-day average $F_{10.7a} = 130$.

[12] The IS radar measurements were conducted from 1300 UT on 21 September to 1500 UT on 25 September. The results of the analysis of the ionosphere processes over Kharkov that accompanied the geomagnetic storm on 25 September 1998 were described in detail in some publications, for example, by *Chernogor et al.* [2002a, 2002b], *Grigorenko et al.* [2003a, 2003b], *Mishin et al.* [2001, 2002], *Taran* [2001], and *Taran et al.* [1999]. Here we consider briefly the main results and their interpretation.

[13] The very strong negative ionosphere storm commenced soon after the local midnight on 25 September and persisted at least until the end of the measurements (here with $K_p \geq 7$). For the Kharkov IS radar ($\lambda = 36.3^\circ E$) local Daylight Saving time corresponds to $LT \approx (UT + 0325)$. The storm was accompanied by a decrease in the peak of the electron density $N_m F2$ during the main magnetic storm phase approximately by a factor up to 3–3.5 as compared to the reference day, for which the data averaged over the previous weakly disturbed days on 21–23 September were selected (Figure 2a). The maximum decrease of $N_m F2$ was observed in the morning time (approximately during 0130–0800 UT). Then $N_m F2$ gradually increased, reached and even exceeded (during short time) the reference values $N_m F2$ near noon, whereupon again began to decrease up to a factor of 1.4 about 1500 UT. The height of the electron density peak $h_m F2$ increased at about 100 km at night and at 50 km near the noon (Figure 2b). In the morning during the main storm phase, the main electron density N_e peak descended to the $F1$ region (below 200 km) where the molecular ions dominate.

[14] To study peculiarities of the ionospheric storm, we consider the vertical profiles of N_e at successive moments of time (every 15 min) during the main magnetic storm phase (Figure 3). Within the time interval of 0430–0830 UT a significant deformation of the $N_e(h)$ profiles was observed: the electron density in the $F2$ -layer maximum decreased, the height and the thickness of the layer increased,

¹For this and other figures the dates are shown at the horizontal axis, fluxes of protons are taken with energies greater than 10, 50, and 100 MeV and of electrons with energies greater than 2 MeV.

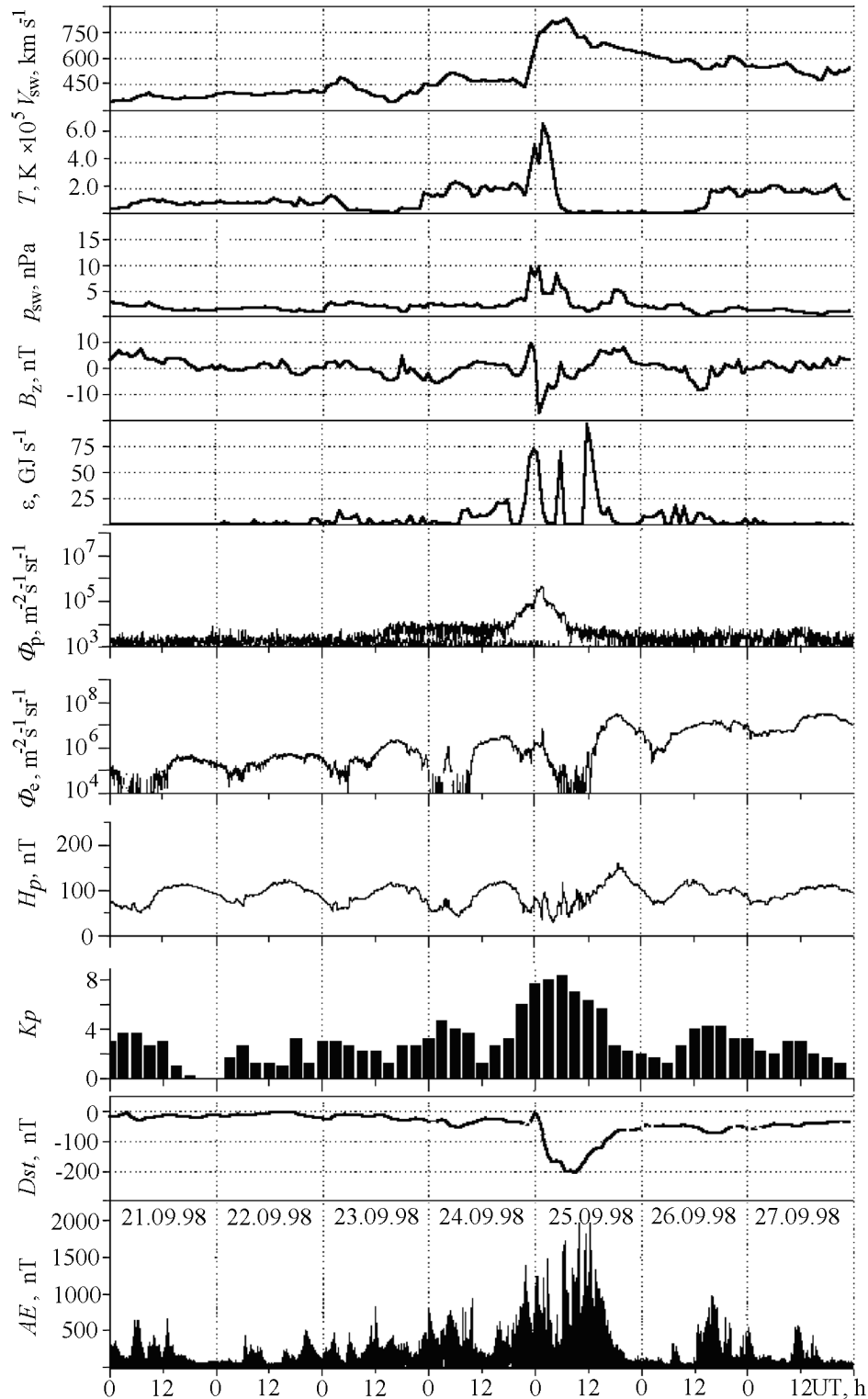


Figure 1. Time variations of the solar wind parameters: radial speed V_{sw} , temperature T (ACE Solar Wind Electron Proton Alpha Monitor), and dynamic pressure p_{sw} (calculation); B_z component of the IMF (ACE Magnetometer), calculated Akasofu function ε (energy transferred by the solar wind to the Earth's magnetosphere per time unit), density of fluxes of protons (GOES 8 (W75)), and electrons (GOES 8), H_p component of the geomagnetic field (GOES 8), the planetary 3-hour Kp index (USAF 55th Space Weather Squadron), Dst index (WDC C2 for Geomagnetism, Kyoto University), and hourly AE index (WDC Kyoto) during the period 21–27 September 1998.

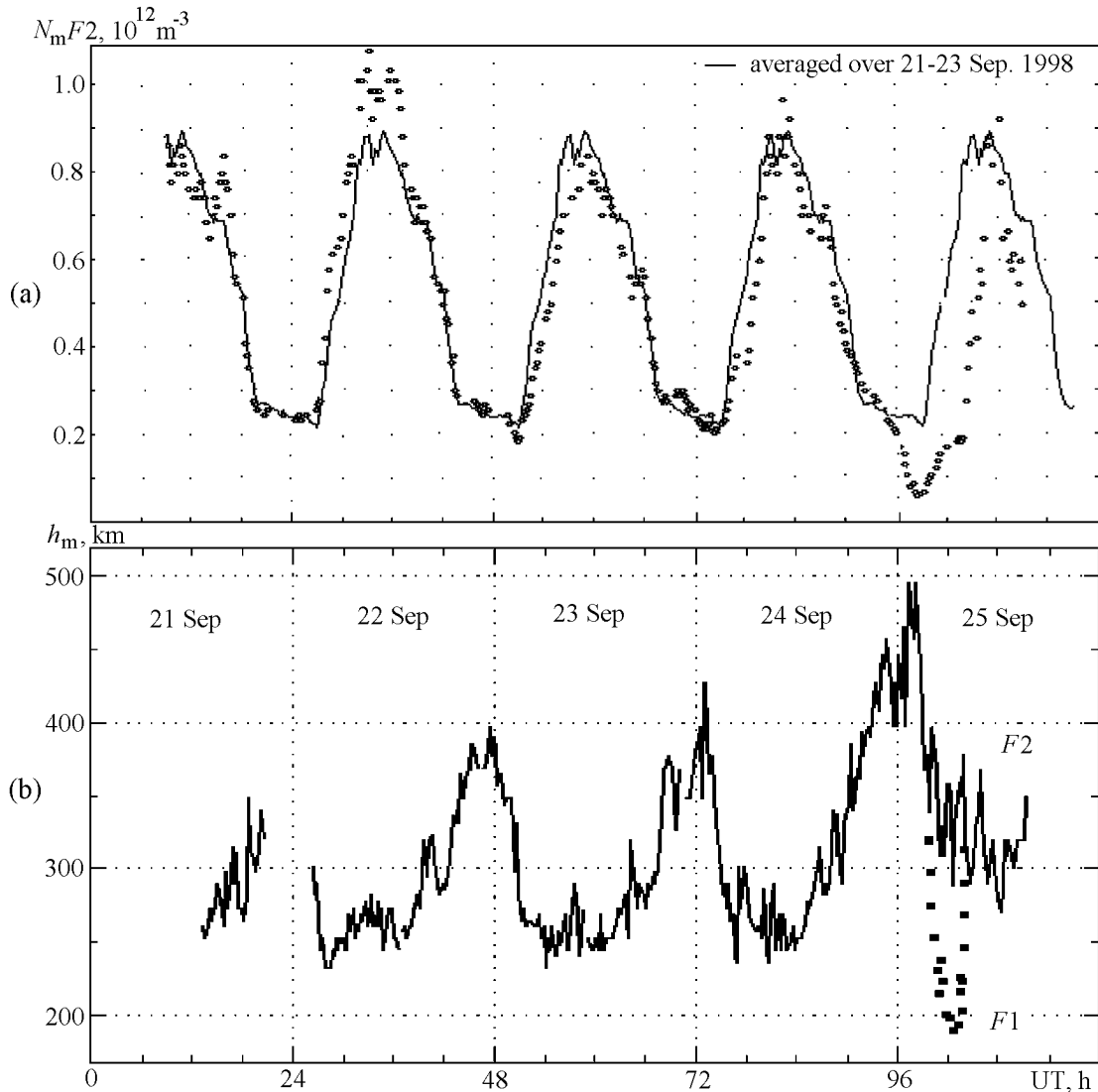


Figure 2. Time variations of (a) the electron density $N_m F2$ at the maximum of the $F2$ layer and (b) the height of the electron density peak h_m above the Kharkov IS radar on 21–25 September 1998 starting from the midnight on 21 September (the height h_m less than 200 km is attributed to the $F1$ -layer peak height). $LT \approx (UT + 0325)$.

and the shape of the profiles changed. These effects could be caused by large-scale disturbance in the neutral composition with a depletion of the ratio $p = N(O)/(N(N_2) + N(O_2))$ and rebuilding in the global thermospheric circulation with an increase of equatorward neutral wind velocity [see, e.g., Brunelly and Namgaladze, 1988; Buonsanto, 1999]. It is known that such events are associated with the high-latitude heating of the thermosphere due to the enhancement of the auroral currents and energetic particle precipitation during the magnetic disturbances [e.g., Danilov and Morozova, 1985; Serebryakov, 1982] that were observed during this storm (see Figure 1). Changes in the neutral composition and thermospheric wind could be also transferred from high to middle latitudes by the traveling atmospheric disturbances (TADs) generated by enhance-

ments of the auroral electrojets during magnetospheric substorms [see, e.g., Buonsanto, 1999; Prölss, 1993a, 1993b, 1995]. Such substorms with the increase of index AE up to about 2000 nT were registered during the main phase of the storm in consideration (see Figure 1, where hourly AE index values are taken). For example, at night on 24–25 September in the absence of ionization production sudden rises in the height of the $F2$ layer were observed at about 2230, 0100, and 0200 UT (see Figure 2b). One can suppose that they are associated with pulse-like increases of the AE index that reached the values of 1400, 2000, and 1600 nT at about 2145, 2345, and 0030 UT, respectively (see (<http://swdcwww.kugi.kyoto-u.ac.jp/index.html>), and AE index values with 1-min time resolution). A similar case was considered, for example, by Prölss [1993a]. From

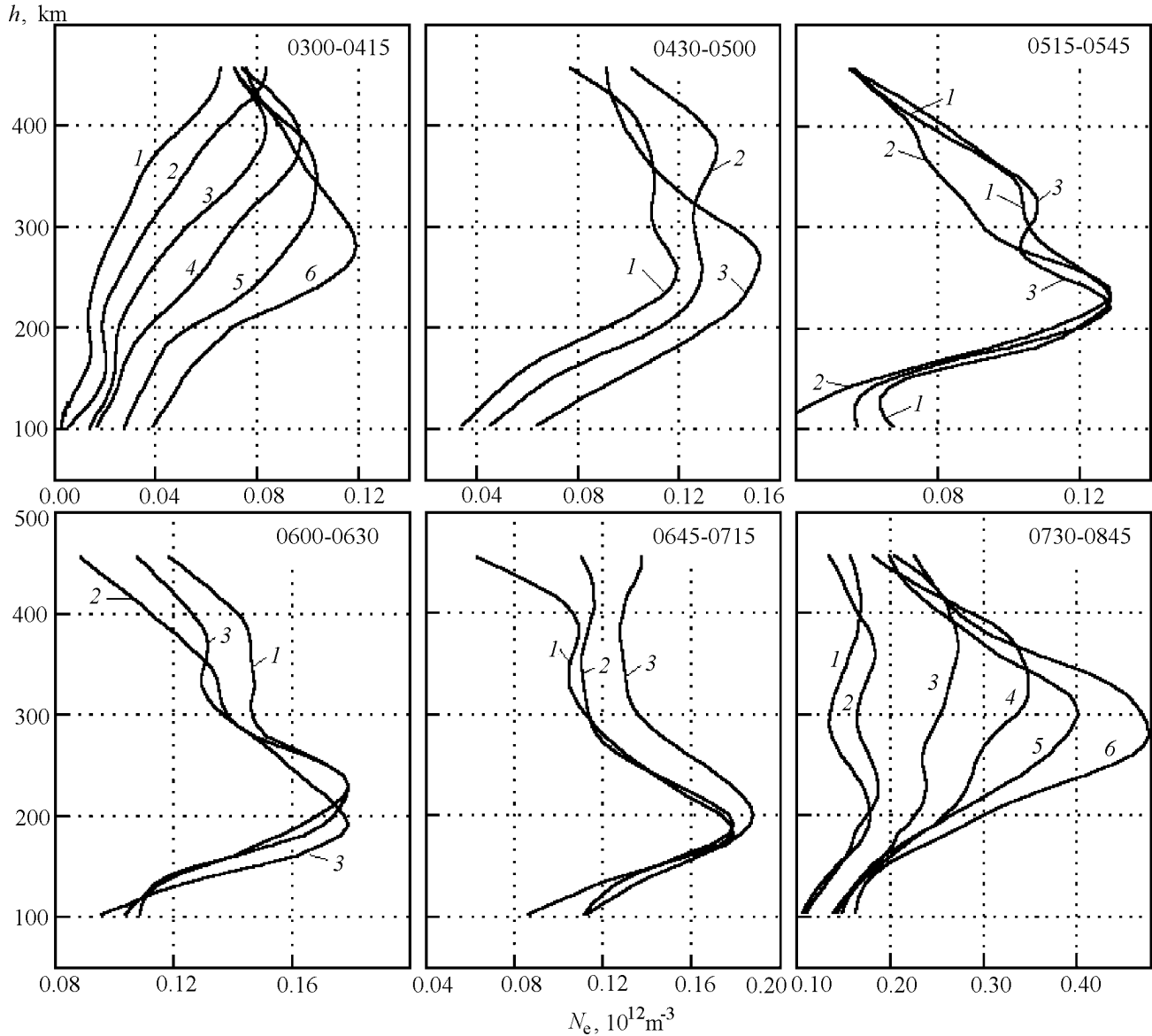


Figure 3. Vertical profiles of the electron density N_e during the disturbed day 25 September 1998 at the consecutive moments of time (each 15 min).

the observed time delay in the disturbances of $h_m F2$ height (of about 45, 75, and 90 min in these cases) and under assumption that the maximum of the source of high-latitude heating occurs near 70° , i.e., at a distance of approximately 2000 km from the Kharkov radar, one can obtain the velocities of TAD propagating toward the equator of about 740, 440 and 370 m s^{-1} , respectively. Such values are typical for the horizontal phase velocity component of the internal gravity waves (IGWs) related to the large-scale TADs.

[15] In the course of the $F2$ -layer deformation, the density N_e in the $F1$ layer varied slightly. As a result, the $N_m F2/N_m F1$ ratio became less than 1 over 0630–0730 UT. The so-called G condition happened, when in ionograms the $F2$ layer was shielded by the $F1$ layer ($f_o F2 \leq f_o F1$). Simi-

lar effects were described, for example, by Buonsanto [1995a] and Mikhailov and Foster [1997].

[16] The simulation using the NRLMSISE-00 empirical model of the atmosphere [Picone et al., 2002] showed that the development of a deep N_e depression in the ionospheric $F2$ layer and the $F2$ -layer decay (the G condition), only partly could be explained by the changes in the neutral composition. For example, at a height of 300 km in the daytime (around 0730 UT) the parameter p from the NRLMSISE-00 model decreased by a factor of 1.1 as compared, for example, to the quiet day on 22 September (Figure 4), whereas the depletion of N_e was by a factor of 3.8 (see Figure 2a). Thus it is required to attract some additional factors to explain the N_e depression. Among these factors, there can be: a correction

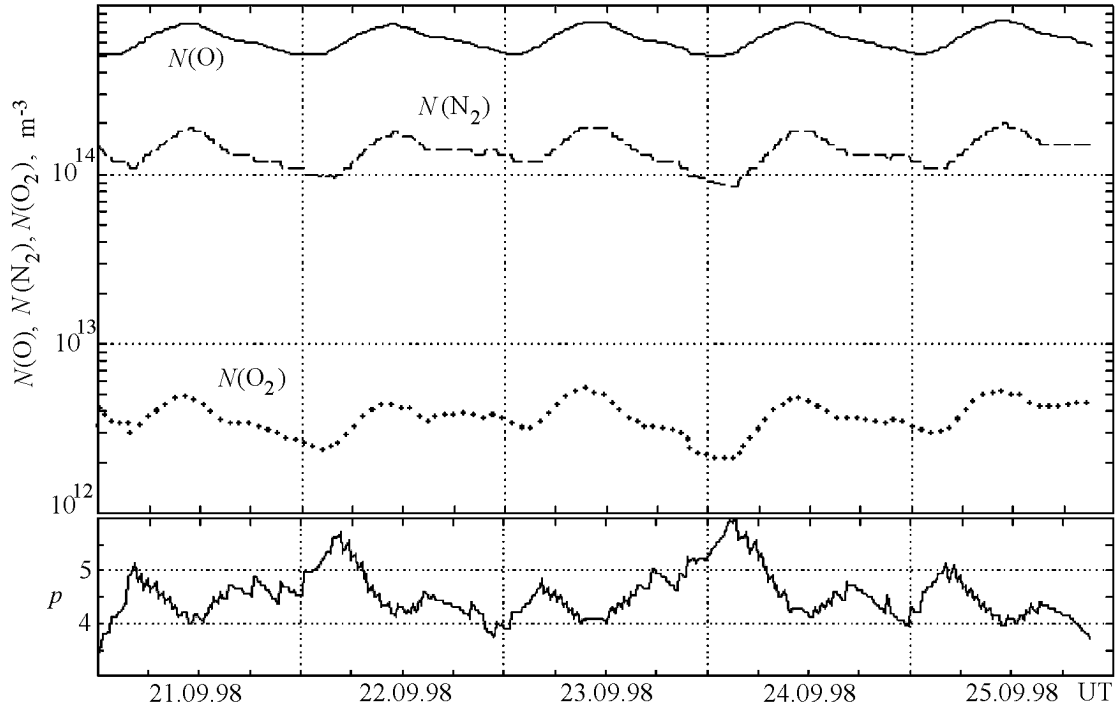


Figure 4. Time variations of concentrations of the main neutral atmospheric components and the parameter $p = N(O)/(N(N_2) + N(O_2))$ at the height of 300 km for the Kharkov radar calculated using the NRLMSISE-00 model.

of the neutral composition taken from the NRLMSISE-00 model for the conditions of geomagnetic disturbances and taking into account possible contribution to the increase of the O^+ ions loss rate of such factors as the atmosphere heating, enhancement of the electric fields, and the excitation of vibrational levels of N_2 and O_2 molecules [Buonsanto, 1995a; Mikhailov and Foster, 1997; Mikhailov and Förster, 1999; Pavlov, 1998; Pavlov and Buonsanto, 1996; Pavlov et al., 1999; Richards et al., 1994; Schlesier and Buonsanto, 1999]. It is known that the character of a magnetic storm is determined by the complicated interaction of a complex of processes in the near-Earth environment. Therefore one should expect that the observed features in the behavior of the disturbed ionosphere are the result of superposition of the effects caused by different disturbance sources, and their contribution changes during the storm. One of such sources (together with the mentioned above) could be the equatorward shift of the main ionospheric trough caused by the enhancement of the electric field of the magnetospheric convection during the main phase of the magnetic storm. The trough shift is confirmed by the analysis of the maps of global distribution of the total electron content (TEC) obtained from the GPS navigation system data [Afraimovich et al., 2002]. It follows from this analysis that on 25 September during the main phase of the storm, the low-latitude wall of the trough in the European region reached a geographic latitude $\varphi = 50 - 40^\circ$ and the Kharkov radar could enter into the trough (in the night and dawn sectors).

[17] The time variations of electron T_e and ion T_i temperatures at heights of 250–500 km are shown in the

Figure 5. Under quiet conditions the electron temperature at midlatitudes is determined by a balance between heating by photoelectrons, thermal conduction along the magnetic field lines, and cooling due to collisions with ions and neutrals. After the storm commencement the increase in T_e was noticed. The enhancement in T_e increased with altitude and at ~ 0200 UT and 500 km altitude it reached ~ 700 K as compared to a quiet day on September 23 (see Figure 5). Increase in T_e could be due to Joule heating associated with penetration of magnetospheric electric fields to midlatitudes and energetic particle precipitations, and also decreased cooling due to very low electron density in the morning time [see, e.g., Buonsanto, 1995a]. The shift toward equator of the precipitation zone could be indirectly confirmed by the maximum values of the POES auroral activity level equal to 10, which were registered on board the NOAA POES 12, 14 and 15 satellites on 24–25 September during 2138 UT–1255 UT interval [http://www.sec.noaa.gov/ftpdir/lists/hpi/power_1998.txt]. The statistical pattern describing the auroral oval is appropriate to the Auroral Activity Level determined from the particle power flux observed during the most recent polar satellite pass. The value 10 of this parameter confirms that the equatorward boundary of the auroral oval could shift to geomagnetic latitudes $\phi \approx 51 - 45^\circ$ [http://www.sec.noaa.gov/Aurora/index.html]. Thus the Kharkov radar ($\phi = 45.7^\circ$) that was close to the midnight sector during the storm main phase could be situated within the trough (see above) and not far from the equatorward boundary of the auroral oval.

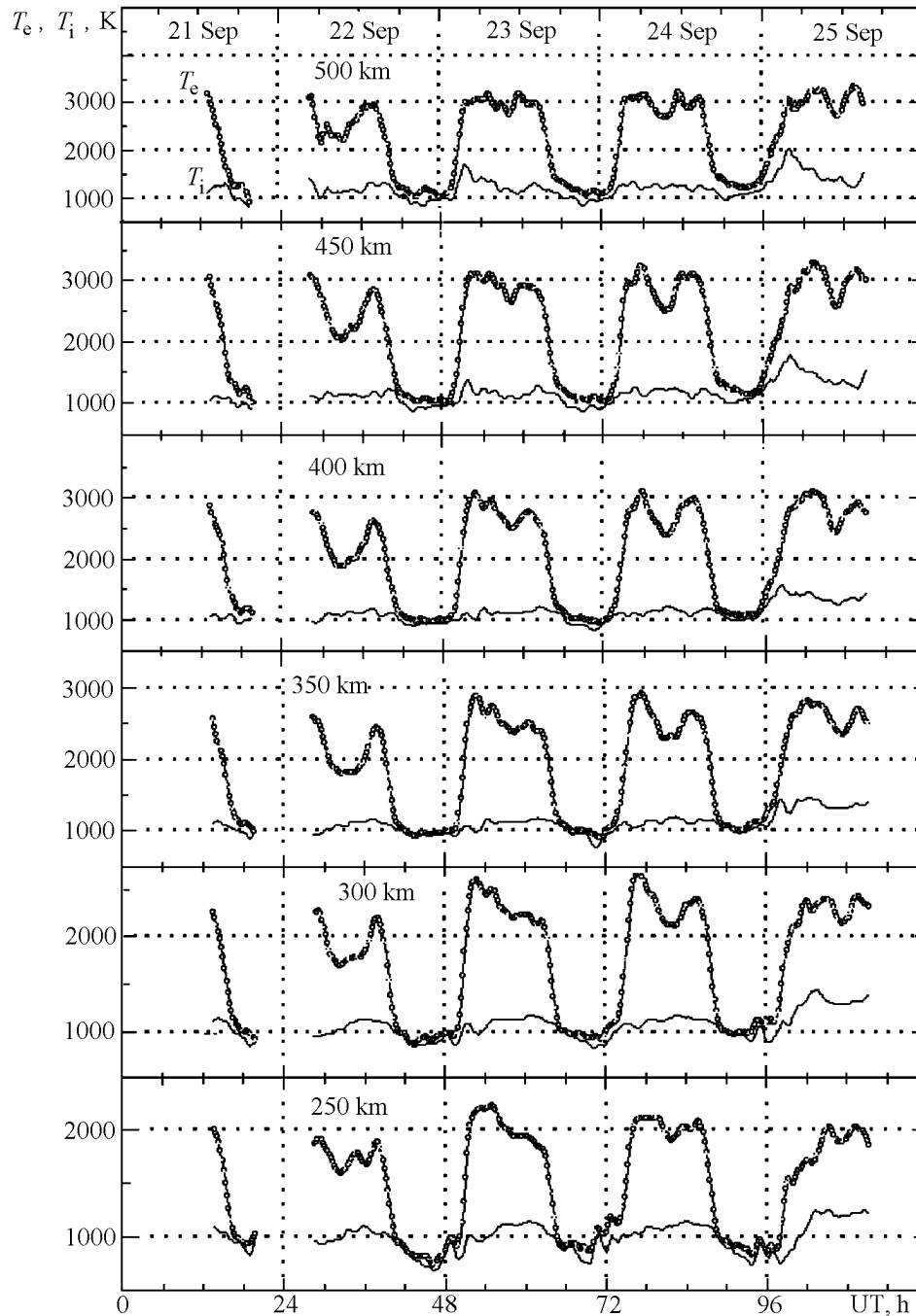


Figure 5. Time variations of the temperatures of electrons T_e and ions T_i at the heights of 250–500 km on 21–25 September 1998.

[18] The peculiarity of the electron temperature behavior was a decrease in T_e after the sunrise (for the Kharkov radar the sunrise was nearly 0325 UT on the Earth's surface) that was by about 500 K at a height of 250 km around 0600 UT and decreased with the altitude growth. This decrease could be caused by several factors, including the intensification of the cooling of the electron gas due to the started morning increase in N_e (see Figure 2a), etc.

[19] Ion temperature under quiet conditions depends on a balance between heating due to collisions with electrons and cooling via collisions with the neutrals. At night, when the heating of electrons is reduced, electron, ion and neutral temperatures tend toward the common value. During this storm the increase in the ion temperature T_i (approximately by 300 K about 0600 UT at 300 km as compared to a quiet day on 23 September) till the end of the mea-

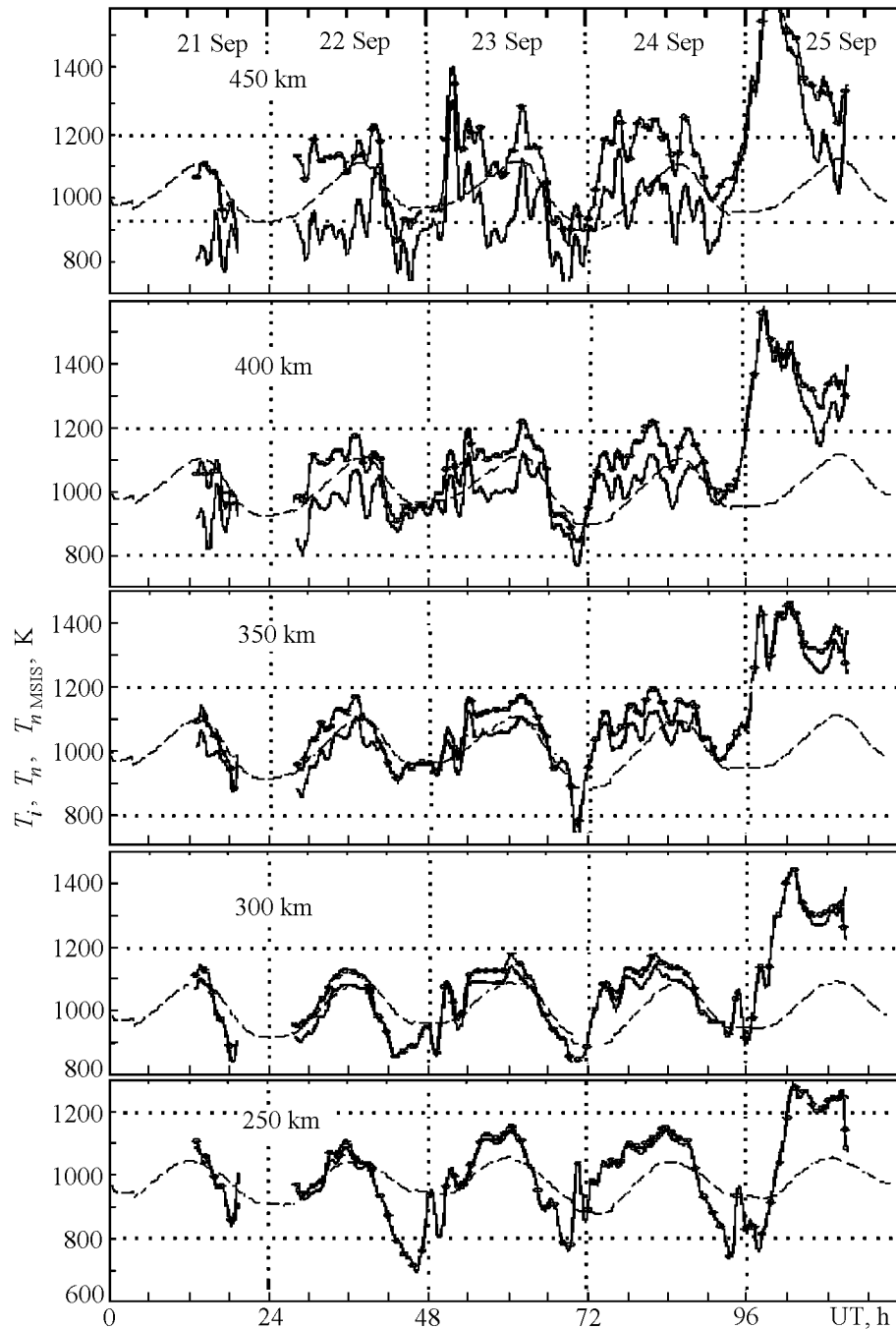


Figure 6. Measured ion temperatures T_i (curve with circles) and neutral temperatures T_n calculated on the basis of the IS radar data (solid curve) and the results of the NRLMSISE-00 model $T_{n\text{MSIS}}$ (dashed curve) at the heights of 250–450 km.

surements (see Figure 5) could be the result of the Joule and the frictional heating associated with the intensification of the ionospheric currents (see below) [Buonsanto, 1995a; Richards *et al.*, 1994].

[20] The temperature T_n of the neutral gas was derived from the IS data by solving the heat balance equation [Salah and Evans, 1973; Salah *et al.*, 1976] and using the

NRLMSISE-00 model of the atmosphere. The calculations showed that during magnetic storm the increase in T_n (Figure 6) was on the average nearly 200 K at a height of 300 km. The heating of neutrals could be related to both, nonlocal source of the heat transported from the region of the high-latitude heating of the thermosphere [Danilov and Morozova, 1985; Mikhailov and Foster, 1997; Serebryakov, 1982] and

local Joule heating due to the penetration of the magnetospheric electric fields to midlatitude (see below) [Mikhailov and Foster, 1997]. Probably both phenomena could occur in the ionosphere over Kharkov during the main phase of the storm. As the obtained results showed (see Figure 6 and Grigorenko et al. [2003b]), the nonlocal heating apparently dominated, because the T_n disturbances were propagating from the above with a velocity of about 50 m s^{-1} (the time delay in the 400–250 km altitude range was about 50 min) and this value could correspond to the vertical component of the IGWs velocity related to TADs. The friction heating due to the ion drift with respect to the neutral gas could provide also some contribution to the increase of T_n during the electric field enhancement over radar [Buonsanto, 1995a]. It should be also noted that the NRLMSISE-00 model (see Figure 6) and MSIS 86 model [see Grigorenko et al., 2003b] give underestimated values of T_n (at a height of 300 km by 450 and 350 K, respectively) in disturbed conditions and require correction. This disagreement (with MSIS 86 model) has been also noted by other authors [see, e.g., Buonsanto, 1995a; Mikhailov and Förster, 1999; Richards et al., 1994].

[21] It should be noted that during quiet days T_n at the heights of 250 and 300 km, apparently, reached the exospheric temperature value and changed slightly, whereas above 300 km the calculated T_n value decreased with the height growth (see Figure 6). This could manifest that the method applied for calculation of T_n at large heights is incorrect and requires taking into account thermal conductivities of ion and neutral gases. At the same time on the disturbed day 25 September thermal conductivity effects can be neglected at least up to the height of 450 km (see Figure 6), that probably can be explained by the disturbance in the neutral composition (increase in N_2 and O_2 concentrations) [Prölss, 1993a, 1993b] (see Figure 4) and in collision frequencies of charged and neutral gas species.

[22] As was mentioned above, the technique we applied to calculate T_i and T_e insufficiently reflects changes in ion composition. Mikhailov and Schlegel [1997] and Mikhailov and Foster [1997] indicated that incorrect consideration of ion composition could result, e.g., in underestimation of T_i and T_e up to 50% during geomagnetic disturbances. Therefore we should anticipate that the calculated values of T_n (as well as other derived parameters, e.g., energy input rate to the electron gas Q/N_e , the heat flux density P_T transferred by electrons from the plasmasphere, etc.) only qualitatively describe the behavior of the disturbed atmosphere.

[23] The mechanisms of the ionospheric disturbance considered above can be attracted for explanation of the observed reversal in the vertical plasma drift velocity and plasma flux during the main phase of the magnetic storm (Figure 7). In the morning hours (near 0400 UT) of the disturbed day, for example, at altitudes 250–350 km, the vertical velocity and flux density of plasma were $V_z \approx 50 - 35 \text{ m s}^{-1}$ and $\Phi_p \approx (4 - 3) \times 10^{12} \text{ m}^{-2} \text{ s}^{-1}$, respectively, whereas on the quiet day (on 23 September) these values were $V_z \approx -(25 - 20) \text{ m s}^{-1}$ and $\Phi_p \approx -(8 - 4) \times 10^{12} \text{ m}^{-2} \text{ s}^{-1}$, respectively.

[24] It is known that at midlatitudes the ion drift velocity is determined by the influence of three mechanisms: ambipolar diffusion along the geomagnetic field lines, neutral

wind and $\mathbf{E} \times \mathbf{B}$ drift of ions. Near the peak of the $F2$ layer where the O^+ ions dominate the vertical ion velocity may be written as [see, e.g., Brunelly and Namgaladze, 1988]

$$V_z = (V_{d\parallel})_z + (V_{n\parallel})_z + (V_{\perp})_z \quad (2)$$

where $(V_{d\parallel})_z$, $(V_{n\parallel})_z$, $(V_{\perp})_z$ are the components of the vertical ion velocity due to ambipolar diffusion, neutral wind and electromagnetic drift, respectively (subscript parallels and perpendiculars relate to the ion velocities parallel and perpendicular to the geomagnetic field induction vector). Substituting the value of each term in the expression (2), we obtain the velocity V_z in the form

$$\begin{aligned} V_z &= V_{dz} + V_{nx} \sin I \cos I \cos D - \\ &V_{ny} \sin I \cos I \sin D + V_{nz} \sin^2 I + \\ &\frac{E_x}{B} \cos I \sin D + \frac{E_y}{B} \cos I \cos D \end{aligned} \quad (3)$$

where

$$V_{dz} = -D_a \sin^2 I \left(\frac{1}{H_p} + \frac{1}{N} \frac{\partial N}{\partial z} + \frac{1}{T_p} \frac{\partial T_p}{\partial z} \right) \quad (4)$$

is the vertical velocity component due to ambipolar diffusion, $D_a = kT_p/m_i \Sigma \nu_{in}$ is the ambipolar diffusion coefficient, V_{nx} , V_{ny} , V_{nz} are the meridional, zonal and vertical components of the neutral wind velocity positive in the north hemisphere when they are directed toward the geographic south, the east and at zenith, respectively, ν_{in} is the ion-neutral collision frequency, $H_p = kT_p/m_i g$ is the scale height of plasma, $T_p = T_e + T_i$ is the plasma temperature, I and D are the geomagnetic field inclination and declination (for Kharkov $I = 66.4^\circ$, $D = 6.7^\circ$); E_x and E_y are the components of electric field intensity vector, directed toward the geographic south and the east in the north hemisphere, B is the absolute value of the geomagnetic field induction vector, m_i is the ion mass (near the peak of the $F2$ layer, predominant ion is O^+).

[25] From the radar measurements of V_z and calculation of the diffusion velocity V_{dz} , the velocity W that includes both electric field and neutral wind effects can be detected:

$$W = V_{n\parallel z} + V_{\perp z} = V_z - V_{dz} \quad (5)$$

If the declination D effects in the expression of V_z (equation (3)) are neglected due to their smallness the velocities $V_{n\parallel z}$ and $V_{\perp z}$ may be written as

$$V_{n\parallel z} \approx V_{nx} \sin I \cos I \quad (6)$$

$$V_{\perp z} \approx \frac{E_y}{B} \cos I \quad (7)$$

In the morning hours (near 0400 UT) on the disturbed day 25 September $W = 100 \text{ m s}^{-1}$ at a height of 300 km, whereas on a quiet day $W \approx 0$ (Figure 8). One of the reasons of this disturbance W and V_z could be equatorward surge in

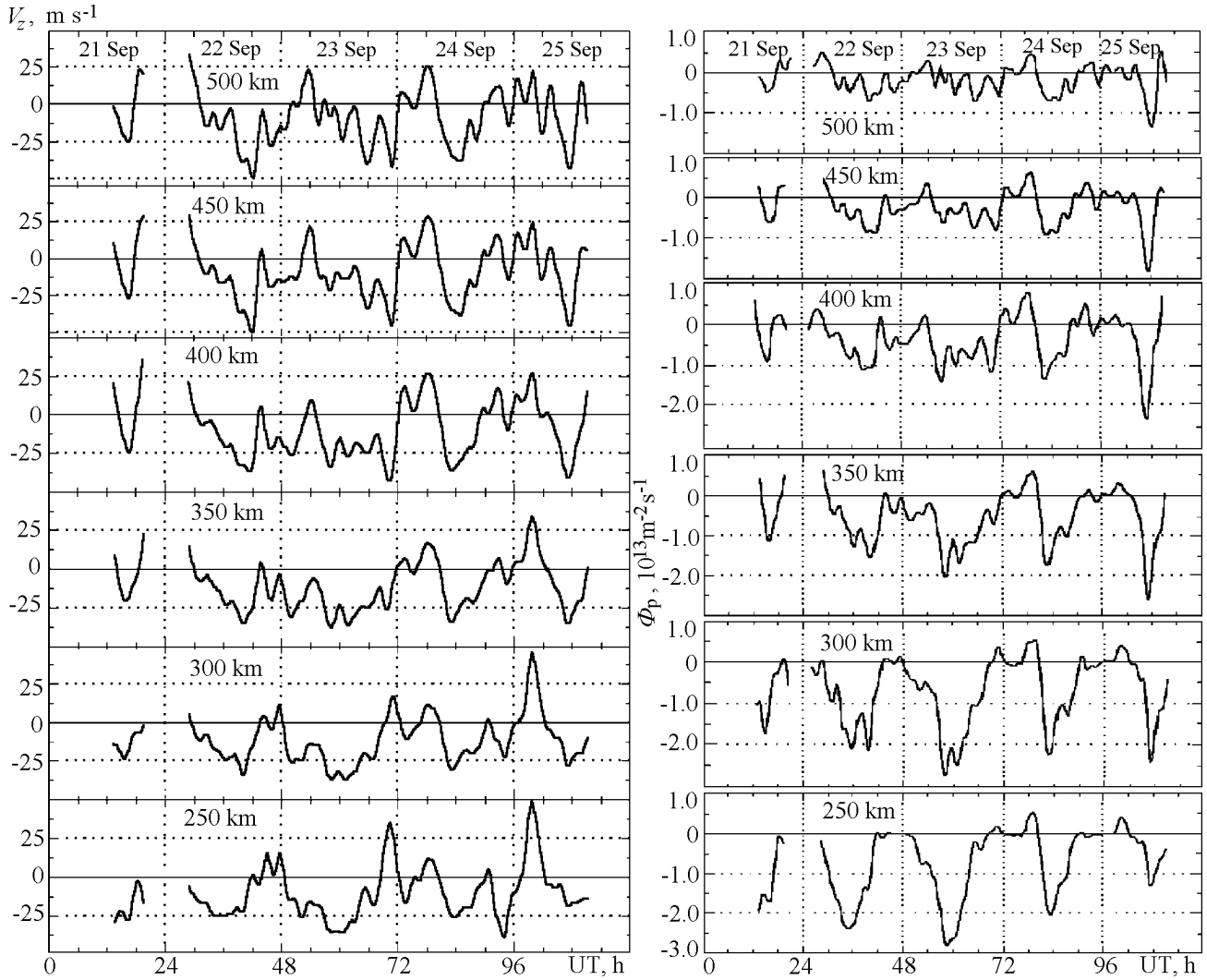


Figure 7. Time variations of the measured vertical plasma drift velocity V_z (left panel) and the calculated plasma flux density Φ_p (right panel) at the heights of 250–500 km on 21–25 September 1998.

the neutral wind V_{nx} caused by the high-latitude heating and TAD [Buonsanto, 1995a, 1999; Buonsanto et al., 1999; Prölss, 1993a, 1993b; Richards et al., 1994]. If the electric fields are neglected, that is correct for the magnetic quiet conditions (as on 21–23 September when $A_p = 14, 10, 14$), the meridional (equatorward positive) component V_{nx} of the thermospheric wind velocity is presented in the form

$$V_{nx} \approx \frac{V_z - V_{dz}}{\sin I \cos I} \quad (8)$$

This velocity should have a value of $\sim 270 \text{ m s}^{-1}$ (see Figure 8). The other reason could be a penetration into mid-latitudes of the nonstationary magnetospheric electric field [Buonsanto et al., 1999; Foster and Rich, 1998; Foster et al., 1998] with the zonal component $E_y = 12 - 17 \text{ mV m}^{-1}$ (determination of E_y from radar measurement of $h_m F2$ see below) capable also to provide $W \approx V_{\perp z} = 100 - 130 \text{ m s}^{-1}$. This case is the limiting one that neglects the neutral wind

effects and gives the upper estimations of E_y and $V_{\perp z}$. In expression (7), $B \approx 5 \times 10^{-5} \text{ T}$ was taken for Kharkov. Probably, both factors contribute to the increase in W and V_z . The high substorm activity (in the auroral region the AE index reached 800–1200 nT at 0300–0340 UT interval) and also the upward propagation of the disturbance in V_z with a velocity of about 100 m s^{-1} (the delay of the disturbance in V_z at 250–500 km altitude range was about 40 min; see Grigorenko et al. [2003b] and Figure 7) could testify to the predominance of the electric field pulse effects over Kharkov. The disturbance in V_z could be caused by the local Joule heating of the atmosphere at the dynamo-region heights (100–110 km), related to the disturbance in the electric field over Kharkov, and upward motion of the gas (similarly to the high-latitude heating source [Mikhailov and Förster, 1999]). The decrease of V_z with the height growth is likely associated with the dissipation of kinetic energy of gas due to viscosity and thermal conductivity.

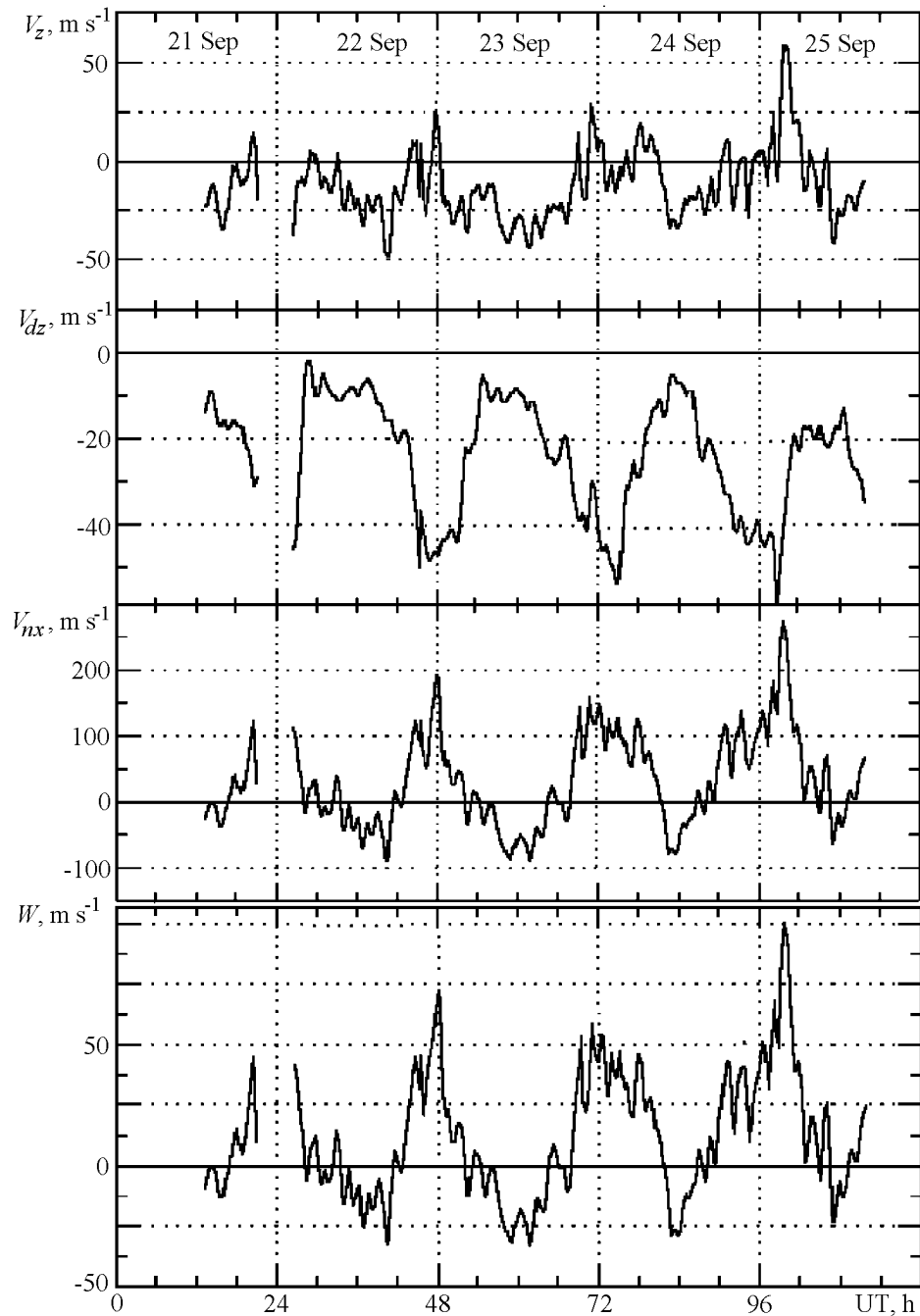


Figure 8. Measured vertical plasma drift velocity V_z (the radar data) and the calculated vertical component of the velocity due to diffusion V_{dz} , meridional component of the neutral wind velocity V_{nx} (neglecting electric fields), and the velocity W at a height of 300 km.

[26] The effects of the electric field penetration (together with the enhancement of the equatorward meridional winds due to the intensification of the high-latitude thermosphere heating source and with the trough shift to midlatitudes) could be one of the reasons of the long-lasting increase in the height of the electron density peak $h_m F2$ by about 100 km at night and 50 km around the noon as compared to the quiet day on 23 September (see Figure 2b). However, these

effects are not related to the nonstationary magnetospheric electric fields as in the case considered above. These effects could be caused by long-lasting precipitation of energetic particles registered during the storm (see Figure 1). Particle precipitations lead to an increase in the conductivity of the underlying auroral ionosphere and short circuiting of the shielding polarization field, and promote a penetration of the magnetospheric electric fields to midlatitudes [see, e.g.,

Brunelly and Namgaladze, 1988; *Gonzales et al.*, 1983]. Estimations of E_y were derived from $h_m F2$ deviations during magnetic disturbances according to simplified empirical dependence given by *Brunelly and Namgaladze* [1988]. They showed that over Kharkov such fields should be eastward directed, should have the values of $E_y \approx 17$ and 12 mV m^{-1} at night and in the daytime, respectively, and can contribute into the observed uplifting of the $F2$ layer.

4.2. The magnetic storm on 29–30 May 2003

[27] The magnetic storm on 29–30 May 2003 was caused by the arrival of two interplanetary shocks from the X1.3 and X3.6 flares on 27–28 May. The main parameters of heliogeophysical situation are presented in Figure 9. The first shock passed the NASA/ACE spacecraft on 29 May at 1150 UT. The second and stronger shock passed ACE at 1830 UT with 125 km s^{-1} increase in the solar wind speed up to over 800 km s^{-1} and B_z deflections that ranged between -20 nT and $+25 \text{ nT}$. The solar wind temperature increased, the dynamic pressure exceeded 15 nPa , ε energy reached the value of 50 GJ s^{-1} at night on 29–30 May. H_p component of geomagnetic field varied in the $0\text{--}200 \text{ nT}$ range. The greater than 10 MeV proton fluxes were observed during several days. The maximum precipitations of electrons began in the premidnight sector on 29 May and continued till local noon on 31 May. Magnetospheric substorms with index AE value greater than 2000 nT were registered during storm. The geomagnetic response to these events was severe storm with maximum indices $Ap = 89$, $Kp = 8+$. The storm commenced suddenly on 29 May about 1225 UT. The main phase developed slowly. The Dst index rapidly decreased to -108 nT at 2300 UT on 29 May and remained at the level of $-(116 - 131) \text{ nT}$ until 0300 UT on 30 May, which was followed by the recovery phase related to northward turn of the IMF B_z component. For this storm solar activity was moderate with $F_{10.7} = 138$ and 117 on 29 and 30 May, respectively, and $F_{10.7a} = 124$. The Kharkov IS radar was operated on 30–31 May according to the international program Low/High Latitude.

[28] The magnetic storm was accompanied by a strong ionospheric storm. Detailed description of the results of observation obtained by the Kharkov IS radar was published by *Grigorenko et al.* [2005a, 2005c]. Substantial effects of a negative ionospheric disturbance were revealed (Figure 10). Among them there were: a depletion of $N_m F2$ by a factor up to 4 during the storm main phase (Figures 10 and 11a); unusual plasma heating at night on 29–30 May when the ion and electron temperatures at altitudes of about $300\text{--}800 \text{ km}$ increased up to the daytime values of $1200\text{--}2400 \text{ K}$ and $2000\text{--}3200 \text{ K}$, respectively, whereas during quiet conditions the values of these temperatures at night were about 800 K (Figures 10 and 12). One of the reasons of these disturbances could be the shift of the main ionospheric trough to midlatitudes and also the shift of the hot zone together with the plasmopause to lower L shells [*Buonsanto*, 1995a, 1995b, 1999; *Richards et al.*, 1994]. Such phenomena in the ionosphere related to the inner plasmasphere (for Kharkov $L \approx 1.9$) occur rarely. The trough equatorward shift was

indirectly confirmed by the maximum values of the POES Auroral Activity Level equal to 10, which were registered on board the NOAA POES 14, 15, 16, and 17 satellites during the storm main phase (approximately from 2223 UT on 29 May till 0233 UT on 30 May) and could manifest the shift of the auroral oval equatorward boundary toward geomagnetic latitudes $\phi \approx 51 - 45^\circ$ (similar to magnetic storm on 25 September 1998). Thus the oval was able to approach the Kharkov radar latitude near local midnight.

[29] It should be noted that we took as a reference data of the averaged values of $f_o F2$ on quiet days 19 and 20 May 2003 obtained by the ionosonde at San Vito (the geographic and geomagnetic coordinates are 40°N , 17°E and 39.7° , 96.4° , respectively), and also the results of ionosphere measurements on 26–27 May 1998 and 23–24 June 1998 (due to the absence of closer quiet periods). The latter periods were on the rising branch of the current solar cycle 23 but similar to the considered period with respect to the parameters of the heliogeophysical conditions (summer, moderate solar activity).

[30] An increase in the $h_m F2$ height by about 160 km during the storm main phase (at night) and by 70 km near noon as compared to reference day on 26–27 May 1998 was registered (Figures 10 and 11b). The lifting of the $F2$ layer is probably explained by the joint action of several factors. They include expansion of the thermosphere, the increase in the equatorward meridional velocity of the thermospheric wind, and the trough shift to middle latitudes. Along with the above reasons, the penetration of magnetospheric electric fields to midlatitudes, similar to the magnetic storm on 25 September 1998, could contribute to an increase in $h_m F2$ due to long-lasting (for more than a day) precipitation of energetic protons and electrons. The latter fact could be manifested in the increase in the flux density of these particles registered on board the GOES 8 and GOES 12 satellites (see Figure 9). In the case when the effects of electric fields are predominant, the maximal values of the eastward zonal field component over Kharkov (determined from the upper E_y estimates obtained based on a change in $h_m F2$) are approximately equal to 25 and 20 mV m^{-1} at night and in daytime, respectively.

[31] It should be referred to an unusual phenomenon that was observed near the sunrise on 30 May. It included a quasiperiodic disturbance in the velocity V_z for about 0200–0400 UT (Figure 13) against a background of the unusual morning decrease in $N_m F2$ (see Figure 11a), a sharp decrease and the following increase in $h_m F2$ by about 160 km (see Figure 11b, the time of these perturbations is shown by horizontal segments), and deformation of the N_e profile (Figure 14) (see *Grigorenko et al.* [2005a, 2005c] for details). One should note that such phenomena also could result from the superposition of the effects of different disturbance sources [see, e.g., *Buonsanto*, 1999]. One of these sources could be the penetration to midlatitudes of the nonstationary magnetospheric electric fields [*Gonzales et al.*, 1983; *Foster and Rich*, 1998; *Foster et al.*, 1998]. Thus an increase in $h_m F2$ by about 90 km at 0330–0400 UT and later (ignoring $h_m F2$ changes due to N_e profile stratification, see Figures 11b and 14) could be caused by a pulse of the electric field in the ionosphere over Kharkov with the eastward

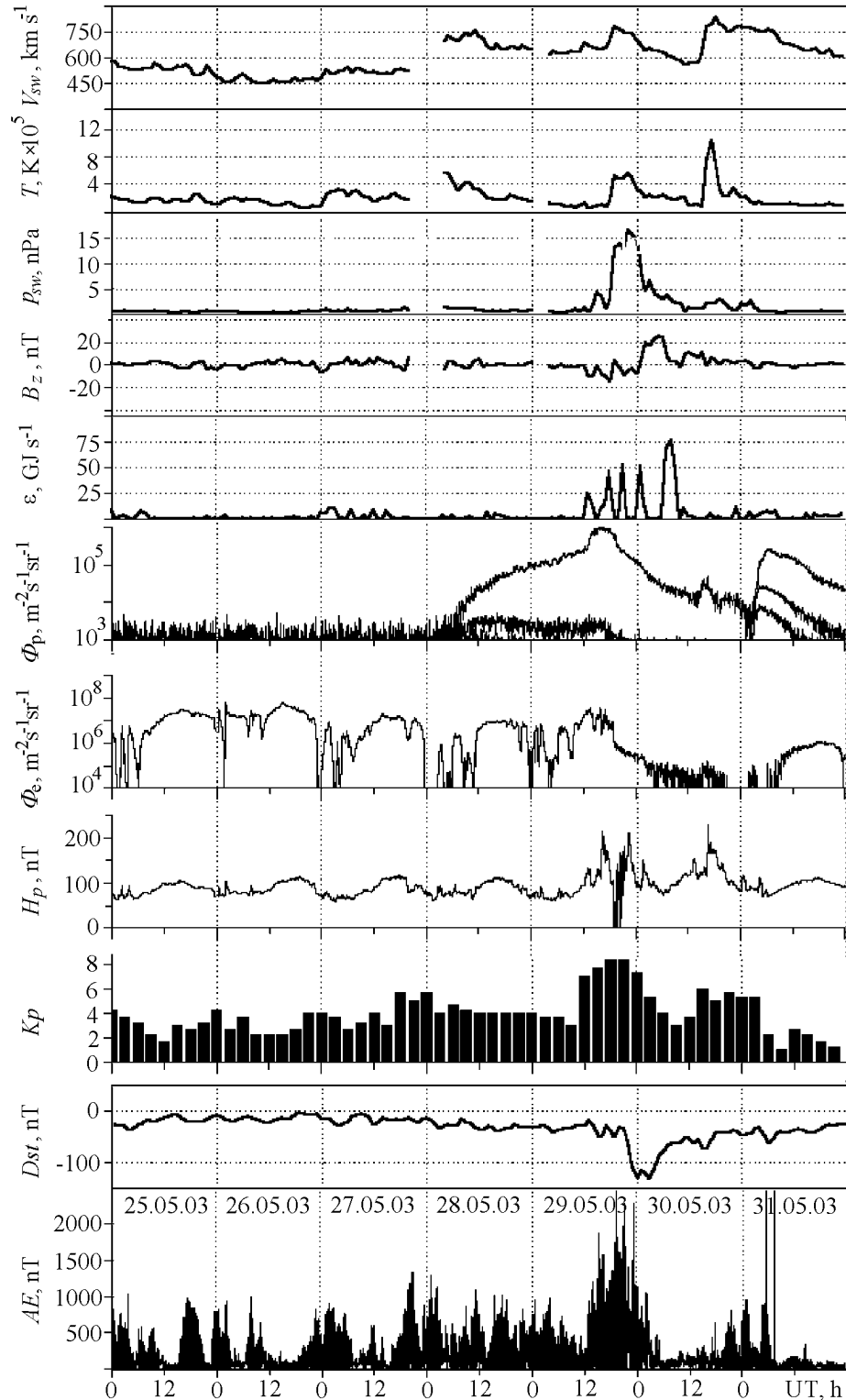


Figure 9. Time variations of the solar wind parameters: radial speed V_{sw} , temperature T (ACE Solar Wind Electron Proton Alpha Monitor), and dynamic pressure p_{sw} (calculation); IMF B_z component (ACE Magnetometer), calculated Akasofu function ε , density of fluxes of protons (GOES 8 (W75)) and electrons (GOES 12), H_p component of the geomagnetic field (GOES 12), the planetary 3-hour K_p index (Air Force Weather Agency), Dst index (WDC C2 for Geomagnetism, Kyoto University), and hourly AE index (WDC Kyoto) during the period 25–31 May 2003.

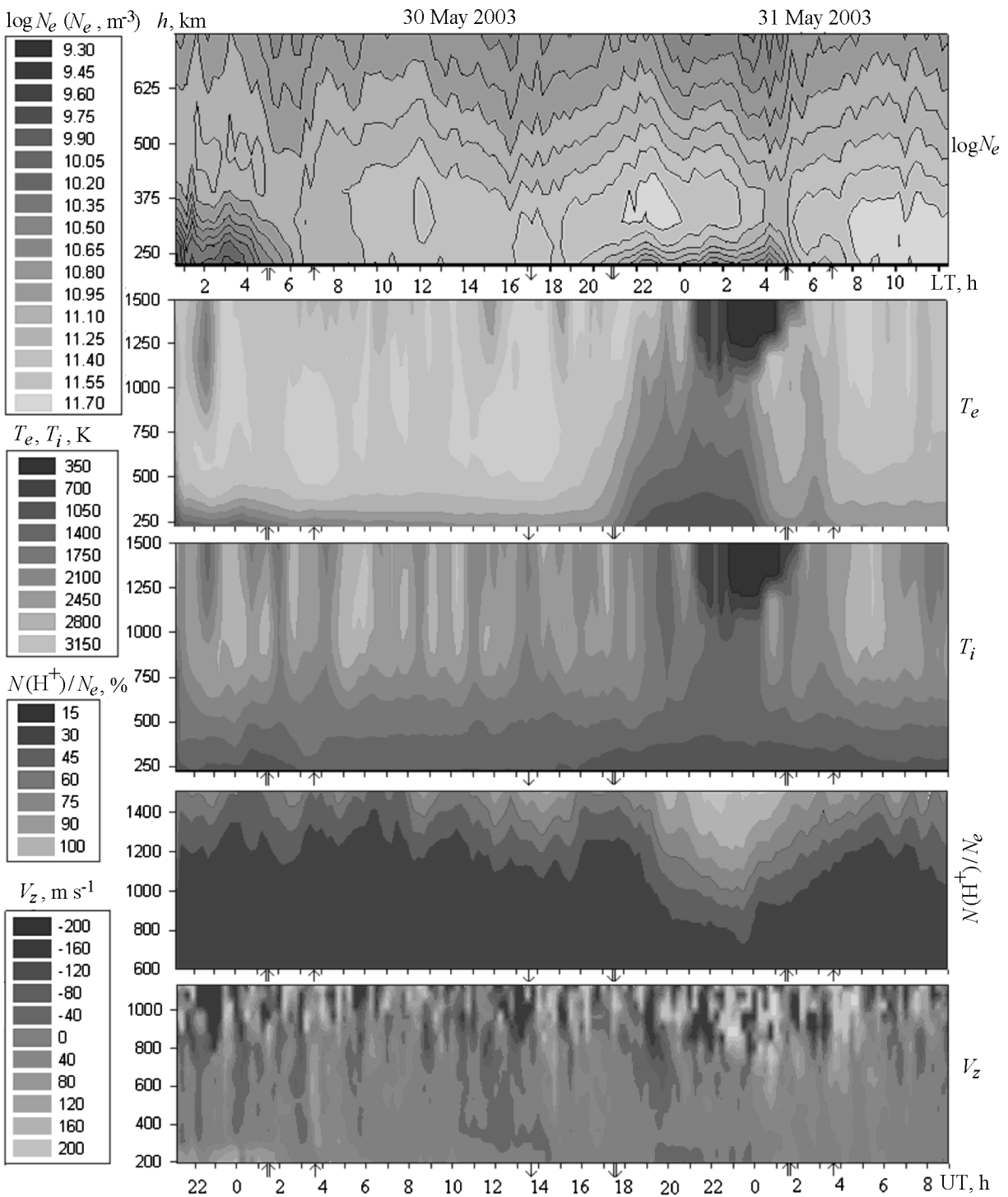


Figure 10. Variations of the ionospheric parameters on 29–31 May 2003: electron density (in $\log N_e$), the temperatures of electrons T_e and ions T_i , the relative density of hydrogen ions $N(\text{H}^+)/N_e$, and the vertical component of the plasma drift velocity V_z . $\text{LT} \approx (\text{UT} + 0325)$. In this image and in subsequent figures, arrows at the abscissa indicate the moments of sunrise (upward) and sunset (downward) at Kharkov (double) and in the magnetically conjugated point (single) at the surface of the Earth. The magnetically conjugated point for Kharkov is located in the vicinity of Madagascar Island.

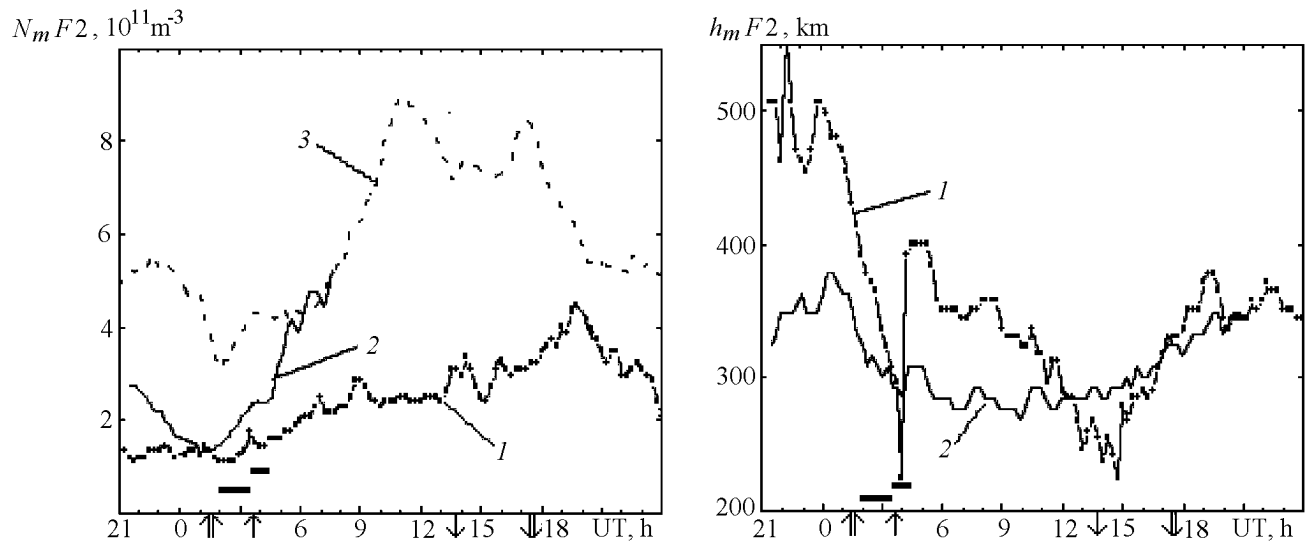


Figure 11. Time variations (left panel) of $N_m F2$ at Kharkov on the disturbed days 29–30 May 2003 (curve 1), on the magnetically quiet day 26–27 May 1998 (curve 2), and on the control day 19–20 May 2003 (according to the data of the ionosonde at San Vito) (curve 3) and (right panel) of the height $h_m F2$ at Kharkov on 29–30 May 2003 (curve 1) and 26–27 May 1998 (curve 2).

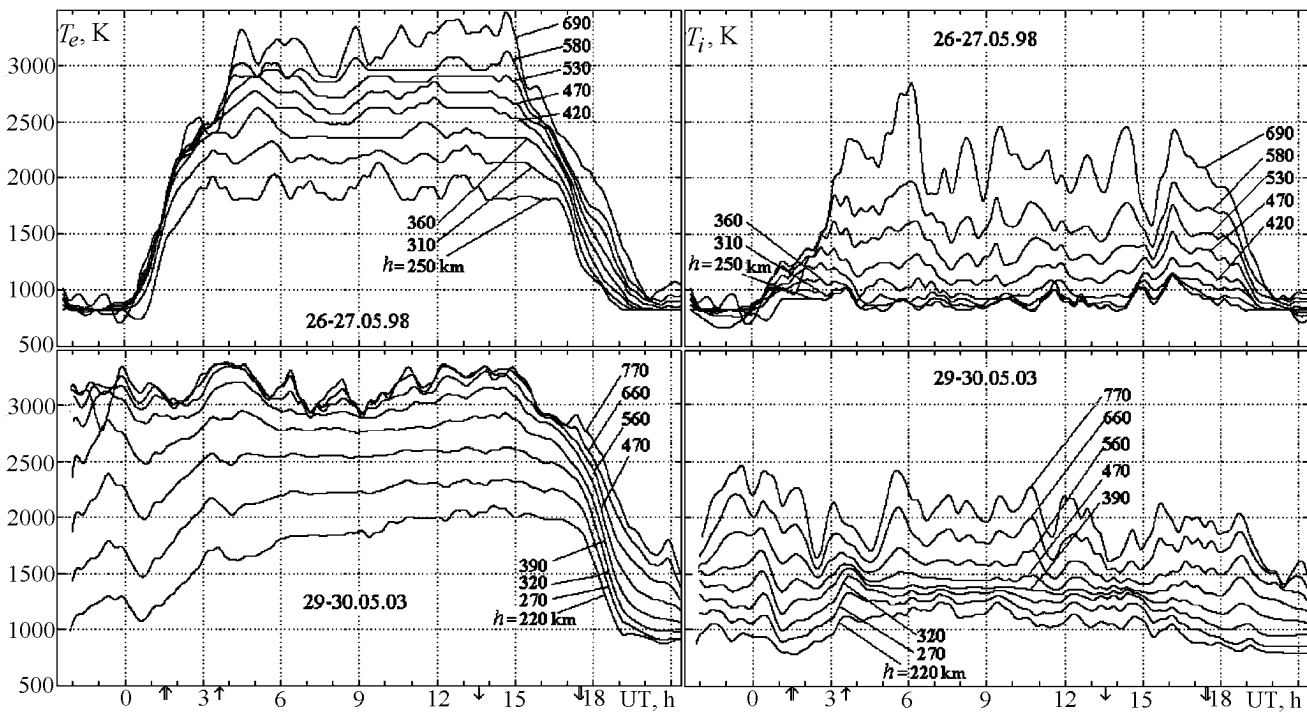


Figure 12. Time variations of temperatures of electrons T_e (left panels) and of ions T_i (right panels) on the quiet day 26–27 May 1998 (top panels) and on the disturbed day 29–30 May 2003 (bottom panels) from the Kharkov radar data.

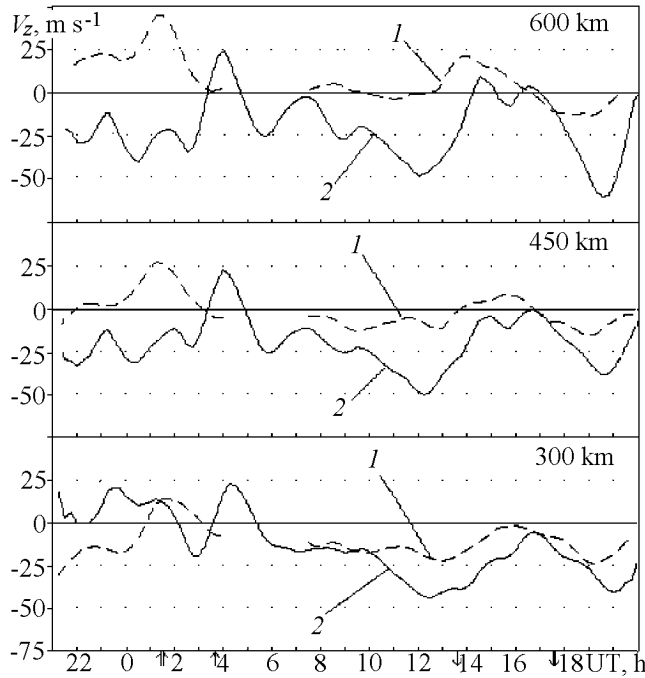


Figure 13. Time variations of the velocity V_z on the quiet day 23–24 June 1998 (curve 1) and on the disturbed day 29–30 May 2003 (curve 2).

zonal component $E_y \cong 20 \text{ mV m}^{-1}$. The sharp turn of the IMF B_z component from the south to the north and change in the dynamical pressure of the solar wind after midnight (see Figure 9) could be the sources of the electric field pulse in the magnetosphere.

[32] The decrease in the relative density of hydrogen ions $N(\text{H}^+)/N_e$ at altitudes of 1000–1500 km more than by an order of magnitude during the storm main phase (at night on 29–30 May), as compared to a reference day on 26–27 May 1998, with its following increase in the daytime on 30 May during the recovery phase (Figure 15) points out the processes of emptying and further filling of the magnetic flux tube over Kharkov radar [Bailey et al., 1979; Brunelly and Namgaladze, 1988; Krinberg and Tashchilin, 1984; Naghmoosh and Murphy, 1983]. The tube is located in the inner plasmasphere and usually is slightly influenced by magnetic disturbances. These effects could be related to the equatorward shift of the main ionospheric trough and the light ion trough and, probably, are accompanied by a change of the processes of ionosphere–magnetosphere interaction. The development of the process of filling in of the magnetic flux tube is defined by a decrease of the height h_t , where $N(\text{O}^+) = N(\text{H}^+)$ (Figure 16). At night on 30 May, h_t exceeded 1500 km and on 31 May h_t decreased down to near 1000 km. During quiet conditions $h_t \approx 700 - 850 \text{ km}$, that is, the h_t height did not reach the level preceding the

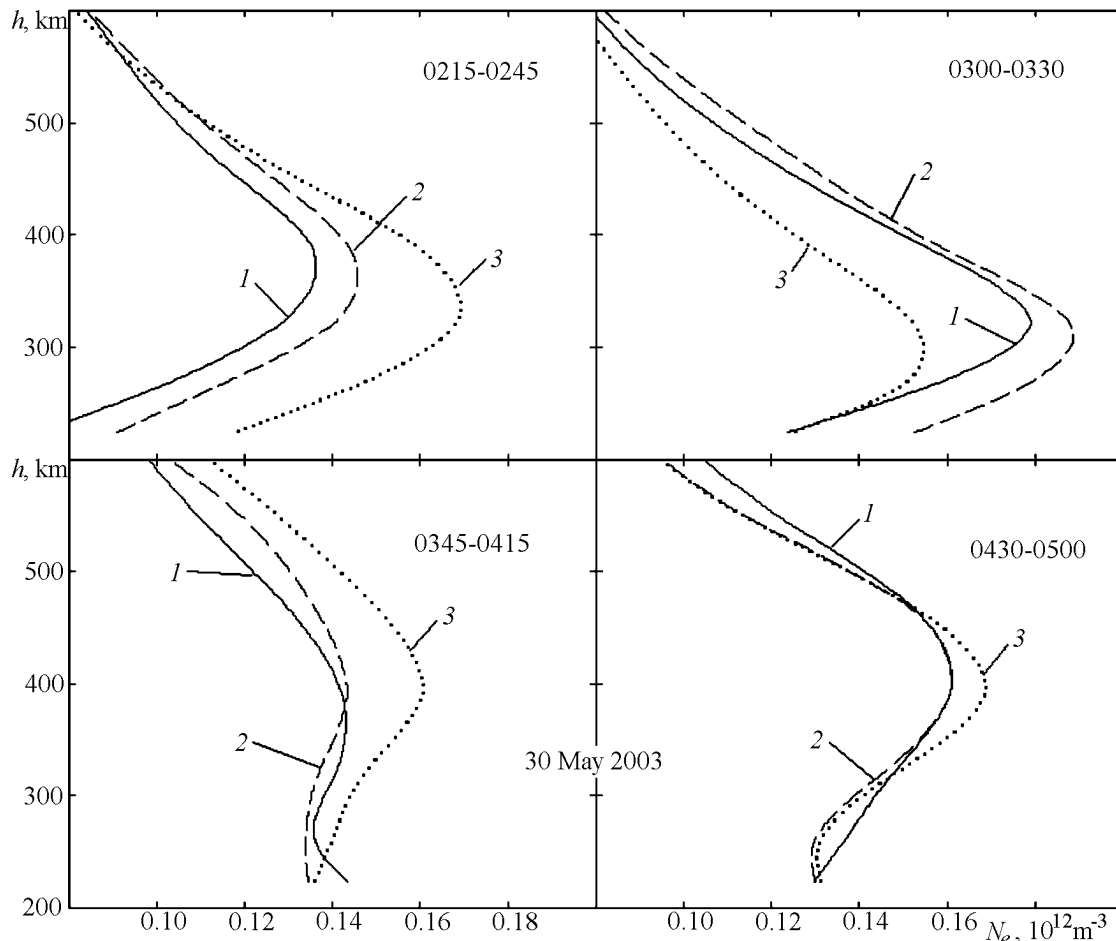


Figure 14. Vertical profiles of electron density N_e at the dawn period of the disturbed day 30 May 2003 in subsequent moments of time (every 15 min).

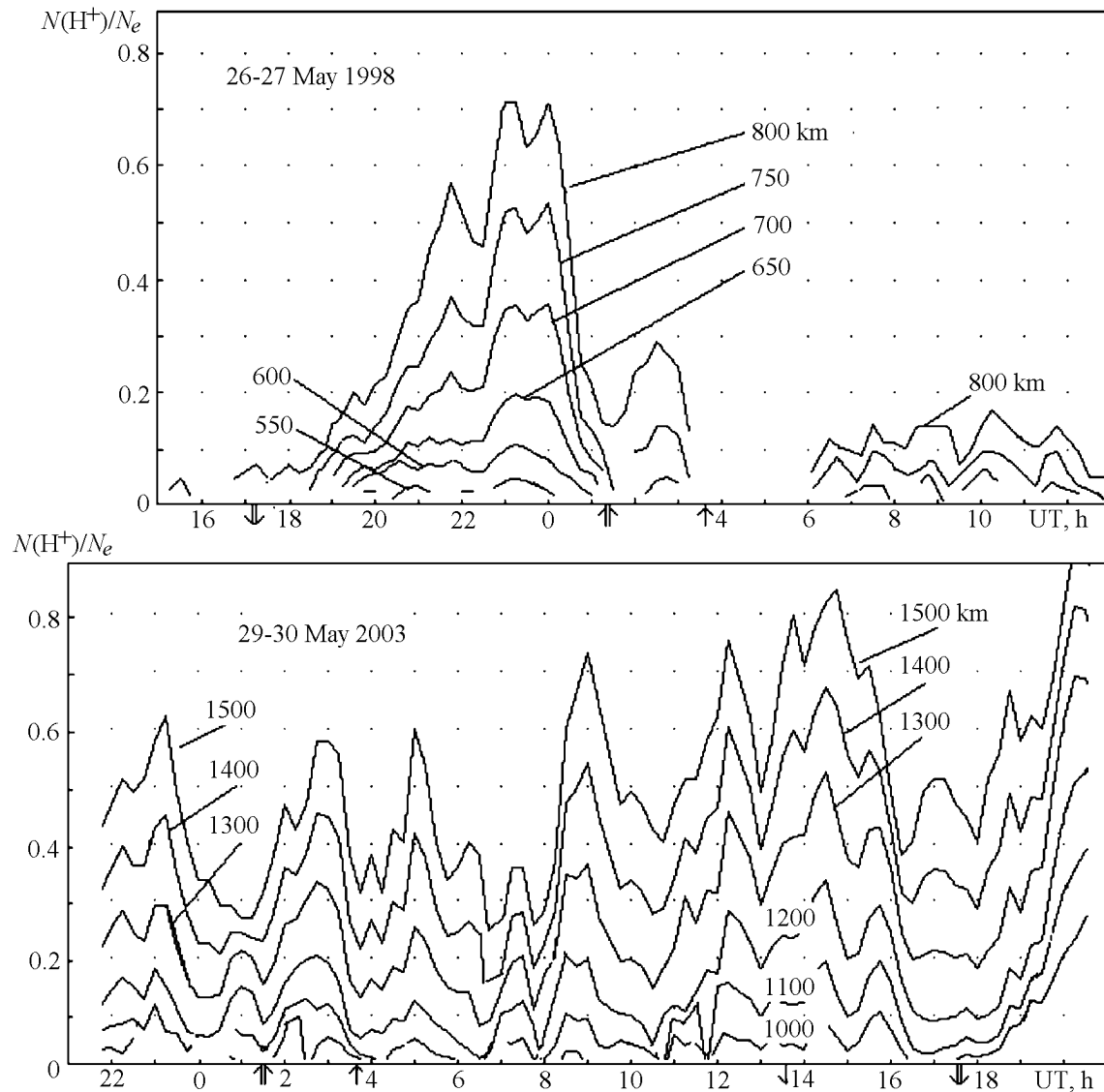


Figure 15. Variations of the relative density of hydrogen ions $N(\text{H}^+)/N_e$ (top) on the reference day 26–27 May 1998 and (bottom) on the disturbed day 29–30 May 2003.

beginning of the storm. It should have been expected, because the process of filling in of magnetic flux tubes proceeds slowly with a time constant proportional to L^4 [Brunnelly and Namgaladze, 1988; Krinberg and Tashchilin, 1984; Saenko *et al.*, 1982].

[33] The magnetic storm was also accompanied by thermospheric disturbances. The calculations using the NRLMSISE-00 model showed that on 30 May, for example, in the daytime about 0800 UT, the changes in the neutral composition led to the depletion of the p parameter by a factor of 1.4 as compared with quiet days on 19–20 May (Figure 17). However, it could not provide the observed for this time depletion of $N_m F_2$ by a factor of 2.5. In the same way as in the case of the 25 September 1998 storm, a correction of the model, or attraction of other factors considered above were required. The distinction of the neutral composition and parameter p during the reference days on 19 and 20 May and before the

storm commencement on 29 May (at 0000–1200 UT) can be explained by the fact that before the reference day the conditions were quiet (for 16–18 May $Ap = 10, 9,$ and 9 , maximal indices $Kp \approx 3$), and for 29 May the conditions were disturbed (on 26–28 May $Ap = 18, 26,$ and 36 , maximal indices $Kp \approx 4, 5,$ and 6 , respectively). It is known that in the model NRLMSISE-00 the values of the 3 hours Ap indices are taken with the “history” (within 72 hours).

[34] The neutral temperature T_n , as calculations showed (see Grigorenko *et al.* [2005a, 2005c] and Figure 18), during the storm main phase ($Kp \approx 8$), when an unusual plasma heating was observed against a background of deep N_e depression in the F region, was about 1000–1350 K at altitudes of 220–470 km, respectively. For comparison, we note that the T_n values decreased by approximately 200–350 K at the same altitudes on the next night during the recovery phase ($Kp \approx 5$). The heating of the atmosphere led to the increase

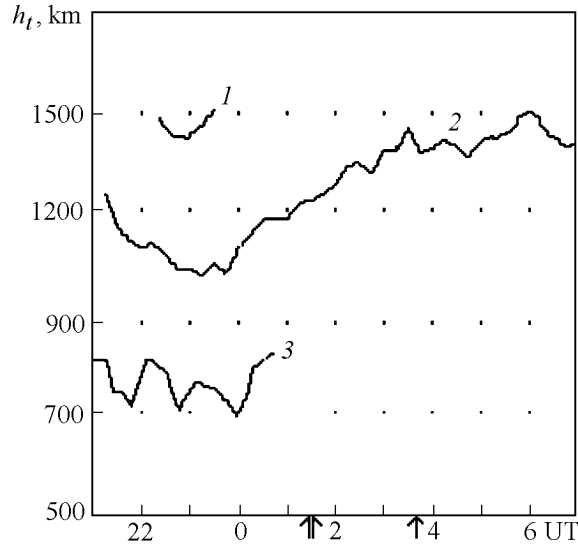


Figure 16. Variations of the height h_t where $N(\text{O}^+) = N(\text{H}^+)$ during the main phase of the magnetic storm on 29–30 May (curve 1), during the recovery phase on 30–31 May 2003 (curve 2), and on a quiet day 26–27 May 1998 (curve 3).

of the thermopause height during the storm main phase at least up to 400 km, whereas on a quiet day its height was about 300 km.

[35] Considerable variations in the thermal regime of plasma accompanied this magnetic storm. The calculations

showed that on the disturbed day about noon, the rate of the energy input to electron gas Q/N_e decreased as compared with a quiet day by a factor of 1.6 (Figure 19). This energy is determined from the thermal balance equation for electrons. Thermal electrons are heated in the process of thermalization of suprathermal electrons, and this process in the lower ionosphere ($h \leq 300 - 350$ km) is local because the mean free paths of these electrons are small. The main mechanisms of electron gas cooling at these altitudes are Coulomb collisions of electrons with ions and excitation of the fine structure levels of oxygen atoms [Banks, 1966; Shunk and Nagy, 1978]. In such a case, the electron energy balance equation in the SI system can be written in the following form for stationary conditions [Banks, 1966; Dalgarno and Degges, 1968]:

$$Q = L_{ei} + L_e \quad (9)$$

$$L_{ei} = 8 \times 10^{-32} N_e^2 (T_e - T_i) T_e^{-3/2} \quad (10)$$

$$L_e = 6.4 \times 10^{-37} N_e N(\text{O}) (T_e - T_i) T_n^{-1} \quad (11)$$

where Q is the rate of the energy transfer to thermal electrons during Coulomb collisions with suprathermal electrons; L_{ei} is the energy loss rate during electron-ion collisions; and L_e is the rate of the energy loss by excitation of the fine structure of oxygen atoms (Q , L_{ei} , and L_e are

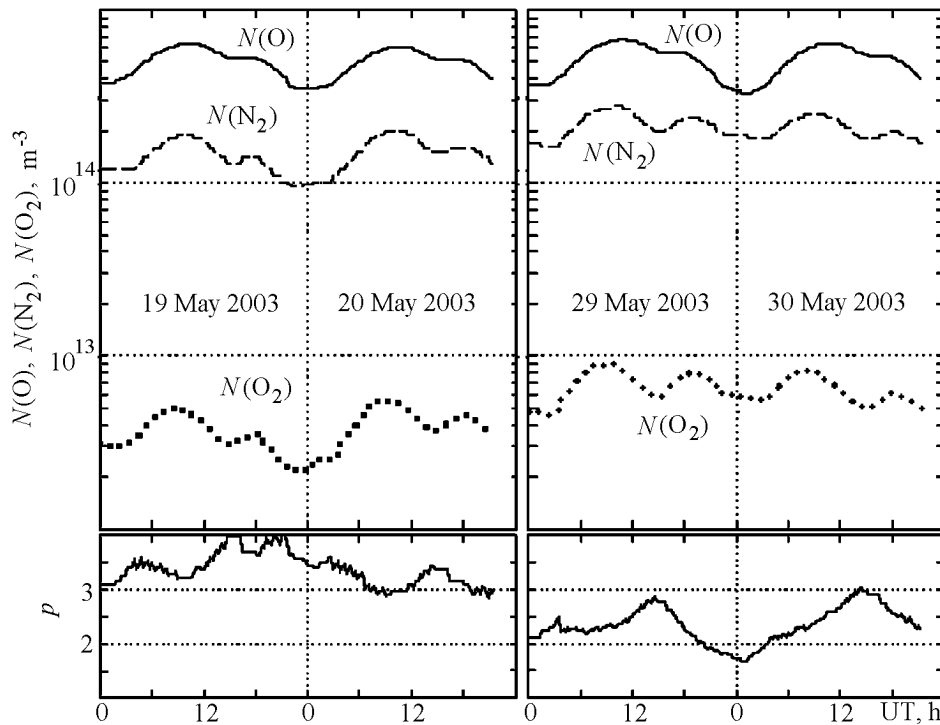


Figure 17. Time variations of concentration of the main neutral components and parameter p at the height of 300 km (left) on the reference days 19 and 20 May 2003 and (right) on the disturbed days 29 and 30 May 2003 (calculated using the NRLMSISE-00 model).

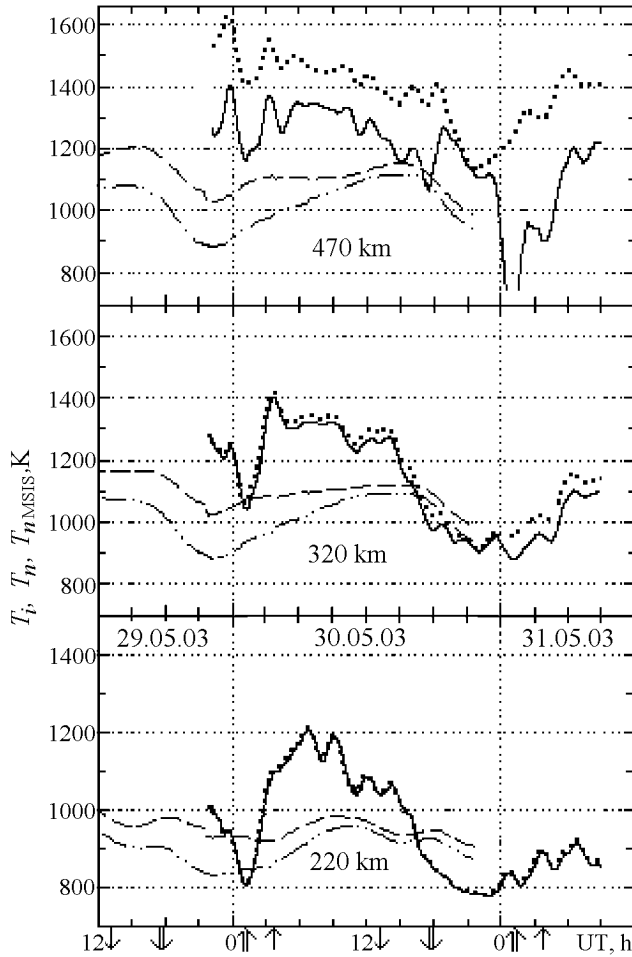


Figure 18. Measured temperatures of ions T_i (dots) and calculated temperatures of neutrals T_n from the IS radar data (solid curves) during the magnetic storm on 29–31 May 2003 and $T_{n\text{MSIS}}$ from the NRLMSISE-00 model (dashed curves) on 29–30 May. The values of $T_{n\text{MSIS}}$ for the quiet days 19–20 May are also shown (dot-dashed curves).

the corresponding energy values per unit time reduced to unit volume). Figure 19 presents results of calculating the Q/N_e energy transferred to electron per unit time, as well as the components of the electron gas energy loss during heat exchange with ions L_{ei}/N_e and neutrals L_e/N_e . Figure 19 indicates that under the quiet and disturbed conditions the contributions of L_{ei}/N_e and L_e/N_e components to the process of electron gas cooling were different.

[36] The decrease in Q/N_e on the disturbed day was accompanied by an increase in the heat flux density P_T , transferred from the plasmasphere due to electron thermal conductivity by a factor of 1.2 (Figure 20). The vertical component of the heat flux density is

$$P_T = -\kappa_e \sin^2 I \frac{\partial T_e}{\partial z}$$

where $\kappa_e = 2.08^2 k N_e T_e / m \nu_{ei}$ is the coefficient of the electron gas thermal conductivity, k is the Boltzmann constant,

m is the electron mass, and ν_{ei} is the electron-ion collision frequency. In the SI system [Ginzburg, 1967]:

$$\nu_{ei} \approx 5.5 \times 10^{-6} N_e T_e^{-3/2} \ln(2.2 \times 10^4 T_e N_e^{-1/3})$$

Substantial values of the energy input rate Q/N_e and the heat flux density P_T during the storm main phase (at night on 29–30 May) became the specific feature of the thermal regime of the ionosphere rarely observed at midlatitudes. Under quiet conditions, these nighttime values were close to zero. These effects manifest the change in the processes controlling the heat balance in the ionosphere–plasmasphere system during a storm [Banks, 1966; Shunk and Nagy, 1978].

4.3. The magnetic storm on 20–21 March 2003

[37] The magnetic storm on 20–21 March 2003 proceeded against a background of high flare activity on the Sun. However, the geoefficiency of the flares was low, and the flares resulted in a minor magnetic storm on 20–21 March 2003 (maximal index $Kp = 5$). Variations in heliogeophysical parameters are presented in Figure 21. After a sudden storm commencement at 0445 UT on 20 March with Dst increasing up to 15 nT at 0600 UT, Dst decreased to -57 nT at 2000 UT. The recovery phase began after 2100 UT and continued till the end of the observations. Solar wind parameters: the temperature and the speed changed weakly, the dynamic pressure did not exceed 4 nT value, the value of the Akasofu function ϵ was less than 30 GJ s^{-1} . The energetic proton fluxes and precipitations of electrons were not practically registered. The variations of the H_p component of geomagnetic field were insignificant. The high substorm activity with the values of index $AE = 1000 - 1500$ nT was observed during the sunset period on 20 March. The storm occurred during moderate solar activity, with the values of index $F_{10.7} = 97$ and 91 on 20 and 21 March, respectively, and an 81-day average value of index $F_{10.7a} = 132$. The measurements were conducted on 19–23 March according to the Storms/TIMED/LTCS program. The radar operated in two-pulse sounding mode in the 100–550 height range with the altitude resolution of about 10 km. The effects of this geomagnetic storm in the ionospheric F region and upper thermosphere over Kharkov were described in detail by Grigorenko *et al.* [2005b, 2005d]. Here we consider briefly the main results of the study.

[38] The magnetic storm was accompanied by a two-phase ionospheric storm (Figure 22a). A peculiarity of the latter was that its strong negative phase occurred against a background of a minor disturbance of the geomagnetic field ($Kp \approx 5$). An increase in $N_m F2$ by about a factor of 1.5 during the positive phase of the storm and a decrease in $N_m F2$ by a factor up to 5 during the negative phase (in the morning hours) as compared to the reference day were registered (Figure 22b). As reference data the $f_o F2$ values were taken during the quiet day on 19 May 2003. They were obtained by the ionospheric stations at Kharkov within 1230–2400 UT and at San Vito within 0000–0730 UT. The information from other (closer) stations was absent for this period. Figure 23

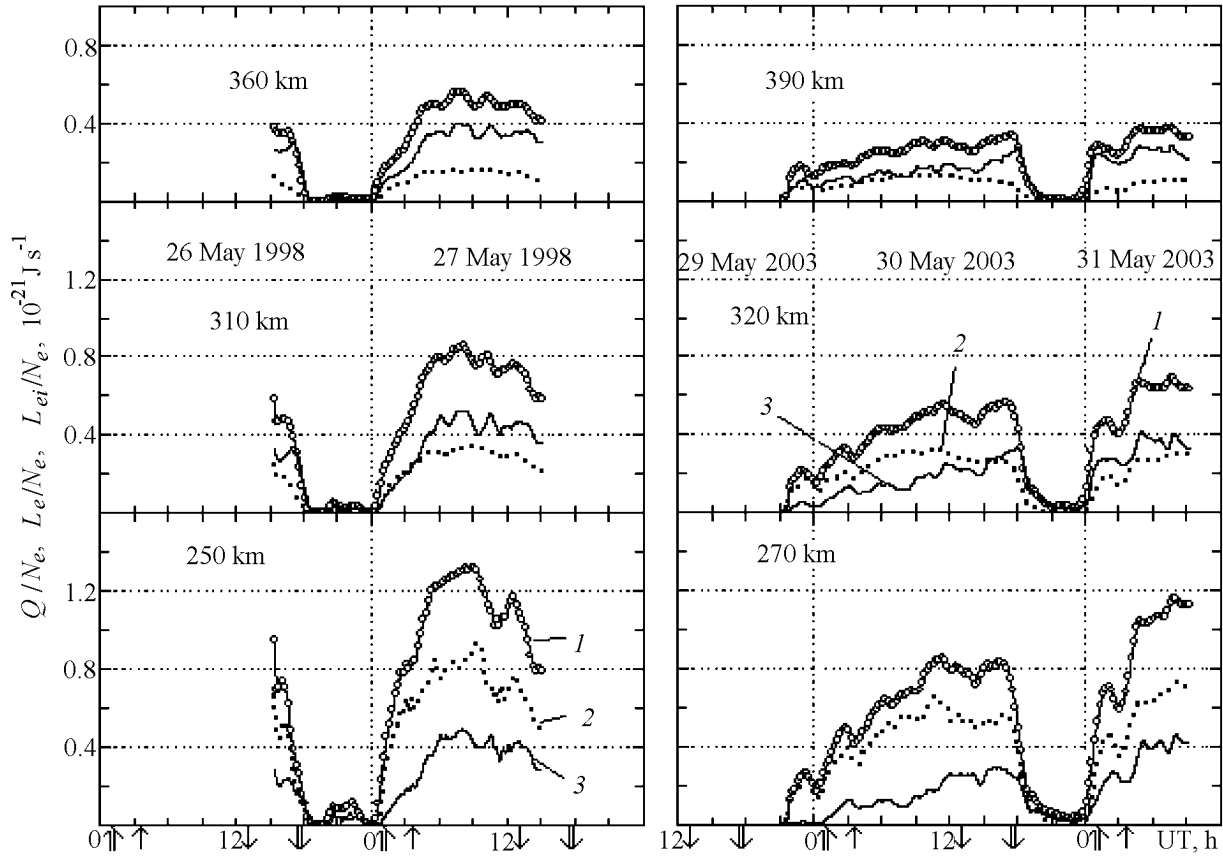


Figure 19. Time variations of the electron gas heating rate (per one electron) Q/N_e (curve 1) and the heat exchange rate of electrons with oxygen atoms L_e/N_e (curve 2) and ions L_{ei}/N_e (curve 3) (left) on the reference day 26–27 May 1998 and (right) during the magnetic storm on 29–31 May 2003.

illustrates the behavior of the electron density N_e and other ionospheric parameters at altitudes of $\sim 100\text{--}550$ km during the storm. A significant distinction of the daytime electron temperatures T_e during the positive (1300 K at an altitude of 300 km) and negative (2400 K) storm phases from the value

$T_e = 1700$ K on a quiet day was detected. The distinction in T_e values during considered days is explained by the different cooling rates of the electron gas in the process of elastic heat exchange with ions, the cooling being proportional to N_e^2 . The ion temperature T_i increase in the daytime at al-

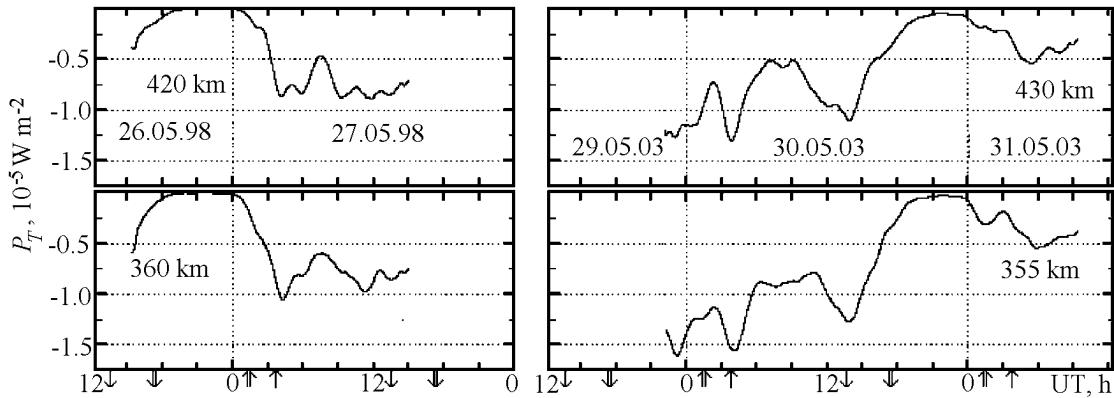


Figure 20. Time variations of the heat flux density P_r transported by electrons from the plasmasphere into the ionosphere (left) on the reference days 26–27 May 1998 and (right) during the magnetic storm on 29–31 May 2003.

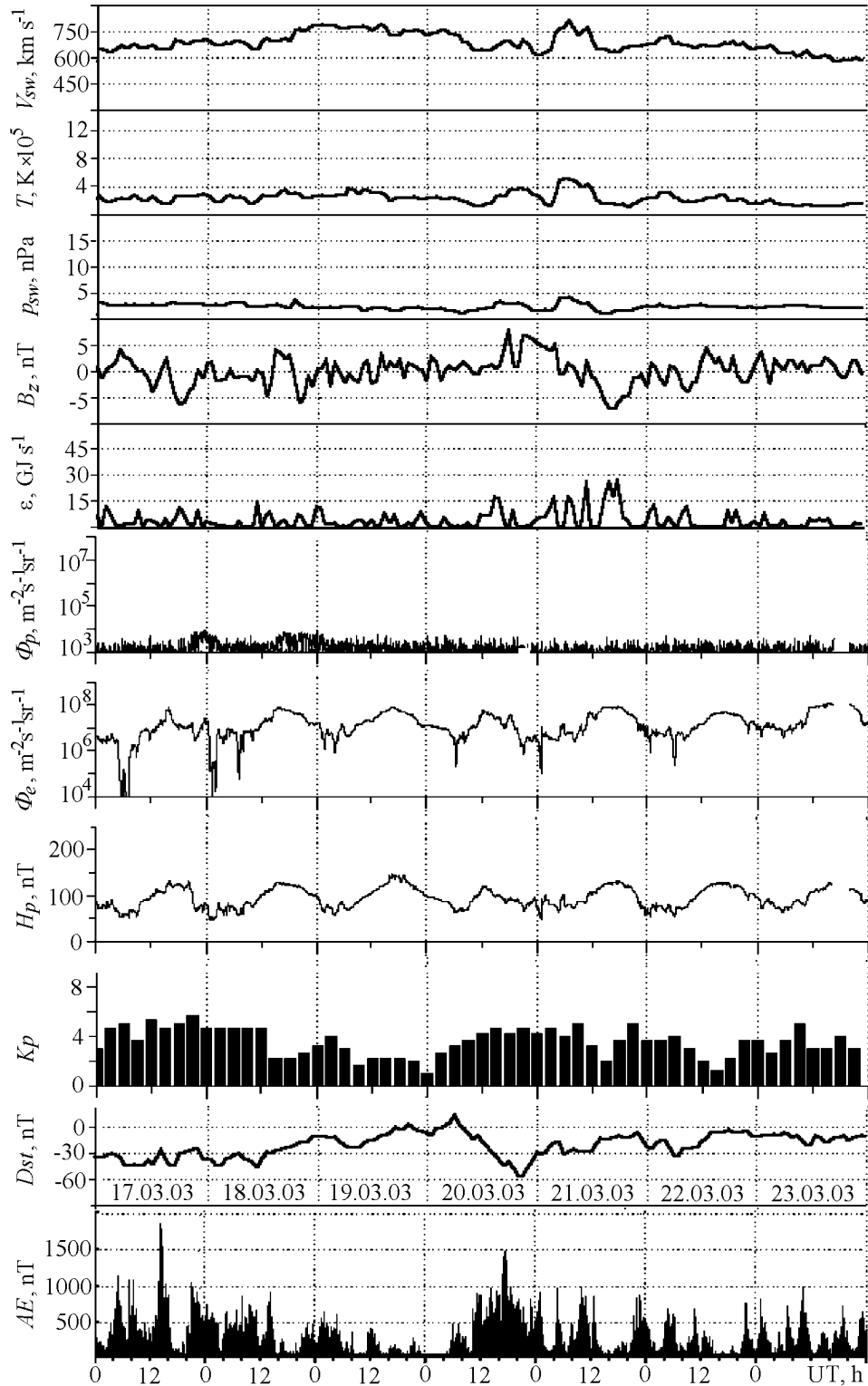


Figure 21. Time variations of the solar wind parameters: radial speed V_{sw} , temperature T (ACE Solar Wind Electron Proton Alpha Monitor), and dynamic pressure p_{sw} (calculation); IMF B_z component (ACE Magnetometer), calculated Akasofu function ϵ , density fluxes of protons (GOES 8 (W75)) and electrons (GOES 12), geomagnetic field H_p component (GOES 12), planetary 3-hour Kp index (Air Force Weather Agency), Dst index (WDC C2 for Geomagnetism, Kyoto University), and hourly AE index (WDC Kyoto) during 17–23 March 2003.

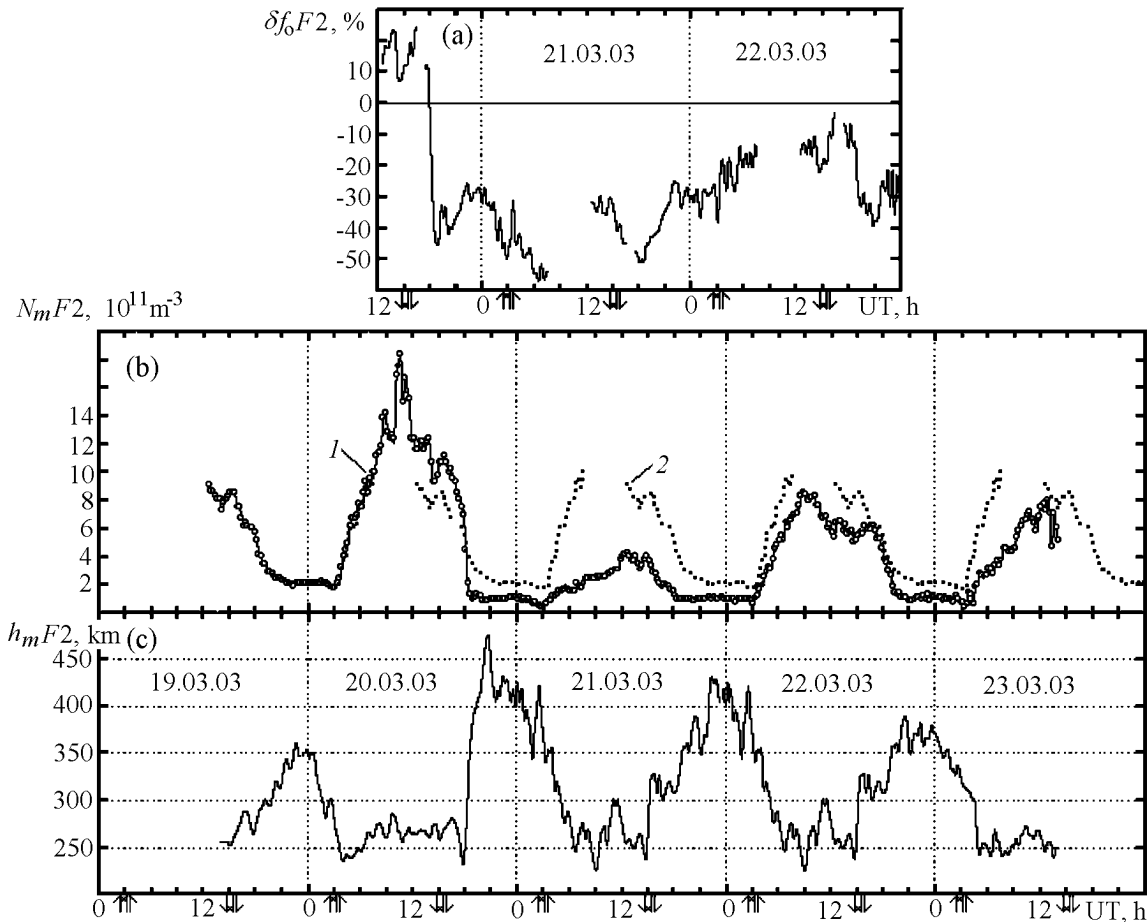


Figure 22. Time variations (a) in the deviations of the critical frequency δf_oF2 measured with the Kharkov ionosonde in comparison with a reference day data during the two-phase ionospheric storm on 20–22 March 2003; (b) in the $F2$ -layer peak electron density N_mF2 calculated for 19–23 March 2003 from the Kharkov ionosonde data (curve 1) and calculated for the reference day 19 March 2003 from the data of ionosondes at San Vito (over 0000–0730 UT interval) and at Kharkov (over 1230–2400 UT interval) (curve 2); and (c) the height h_mF2 of the $F2$ -layer peak from the Kharkov radar data. LT \approx (UT + 0225).

titudes of 250–300 km was about 50 K and 100–150 K on 20 and 21 March, respectively. Apparently, the T_i growth was related to a high-latitude source of atmospheric heating which was not considerable during the minor magnetic storm and also to the increased electron-ion heat exchange due to the substantial difference in the temperatures of electrons and ions on 21 March.

[39] The positive storm phase on 20 March had a character of a long-duration disturbance and lasted approximately for 6 hours. It could be caused by the enhanced equatorward meridional wind V_{nx} , related to the high-latitude thermosphere heating [Buonsanto, 1999; Danilov and Morozova, 1985; Danilov et al., 1985]. A comparison with the quiet period (22 and 23 September 1998 which were chosen as reference days due to absent of any other, more suitable period) indicated that the downward velocity V_z at altitude of 300 km decreased on average by approximately 10 m s^{-1}

near local noon on 20 March 2003 (Figure 24). For Kharkov LT \approx (UT + 0225) in March. If we neglect the contribution of additional electric fields during minor storm and the change of diffusion velocity, we obtain the upper estimate of the $\Delta W \approx 10 \text{ m s}^{-1}$ that lead to the observed increase in h_mF2 by about 20 km. In this case an additional velocity value ΔV_{nx} should be about 25 m s^{-1} .

[40] Let us consider more in detail the processes accompanied the ionospheric storm phase reversal. It occurred in the sunset period and was accompanied by a decrease in h_mF2 by 50 km during 1700–1800 UT with a subsequent ascent of the layer by almost 200 km from 1800 to 1900 UT (Figure 22c). On the reference days of 22–23 September 1998 [see Grigorenko et al., 2003b] and 19 March 2003 (see Figure 22c) a change in the h_mF2 at the sunset was much smaller (about 50 km). At the same time on 20 March, h_mF2 rapidly (for not more than 30 min) decreased by 40 km. Fifteen minutes

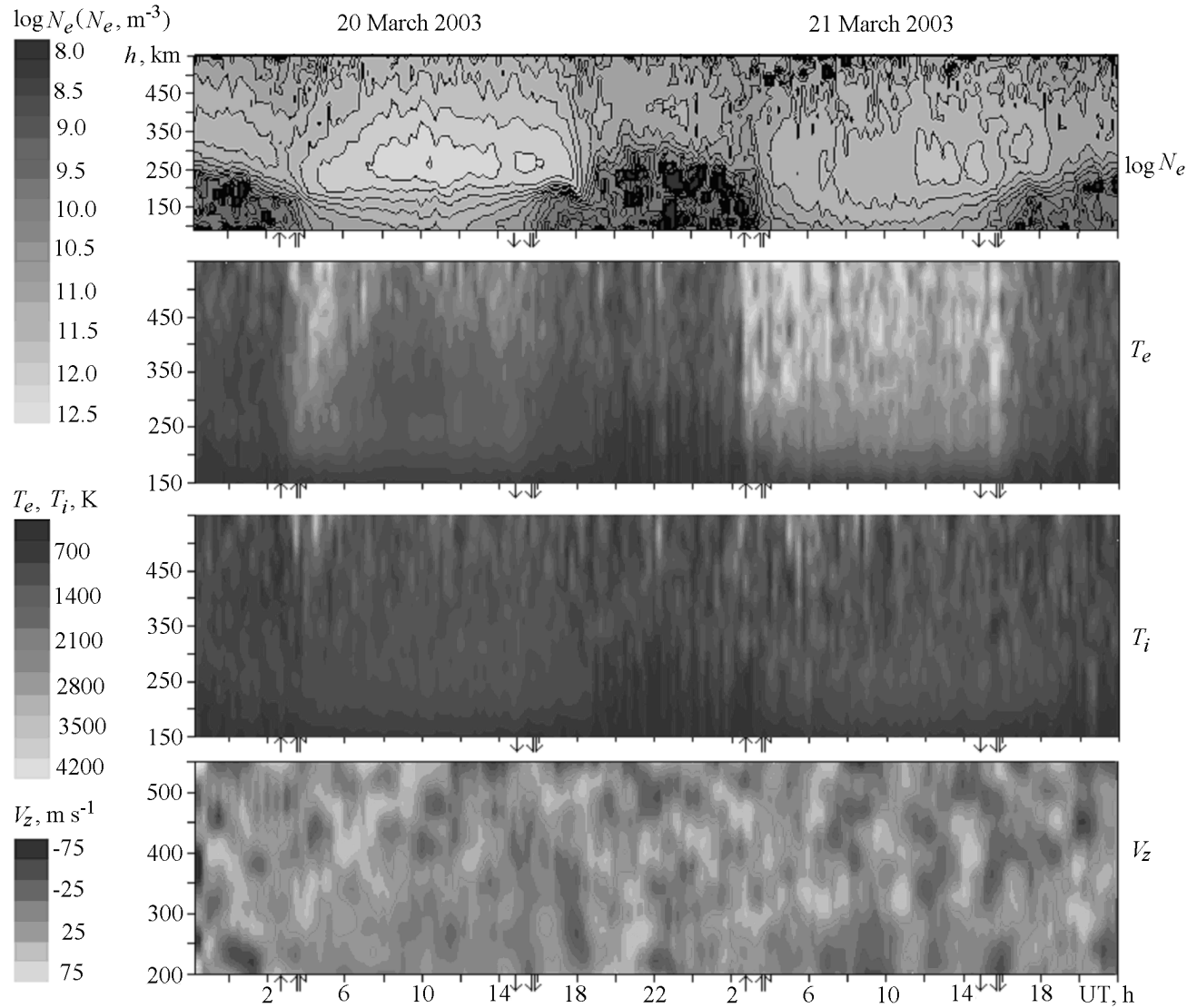


Figure 23. Variations of the ionospheric parameters on 20–21 March 2003: electron density (in $\log N_e$), the temperature of electrons T_e and ions T_i , and the vertical plasma drift V_z .

later, $h_m F2$ increased by about 90 km during one record of measurements, i.e., within 15 min (the data processing was performed at a 15-min signal integration).

[41] It is known [see, e.g., *Foster and Rich*, 1998; *Foster et al.*, 1998] that rapid changes in $h_m F2$ (together with V_z , see Figure 24) can be caused by nonstationary disturbances of magnetospheric electric fields and by the penetration of these fields to midlatitudes. Another mechanism explaining such variations can be related to propagation of TADs generated by an enhancement of auroral electrojets during a substorm [see, e.g., *Prölss*, 1993a, 1993b, 1995]. Such a substorm with a maximal AE value of 1500 nT at auroral latitudes was registered about 1800 UT on the considered day (see Figure 21), i.e., during the ionospheric storm phase reversal. However, TAD effects cannot explain the initial decrease of $h_m F2$ by 50 km since TADs are characterized by the transport of the equatorward meridional wind, as a re-

sult of which the $F2$ layer ascends and $h_m F2$ increases both in daytime and at night. Moreover, TAD (which propagates from the auroral region with a velocity of 400–700 m s^{-1}) appears at midlatitudes with a delay of about 1.5–1 hours. In our case this delay relative to the time of the substorm intensity maximum was almost absent.

[42] Proceeding from the aforesaid, we can assume that an initial decrease in $h_m F2$ could be caused by the penetration into the ionosphere over Kharkov of the magnetospheric electric field with a westward zonal component of $E_y \approx -10 \text{ mV m}^{-1}$. The estimation of E_y value was obtained from the $h_m F2$ variations [*Brunelly and Namgaladze*, 1988]. Such cases of the $h_m F2$ decrease are considered, e.g., by *Reddy and Nishida* [1992] and *Prölss* [1993b] and are explained by increased magnetospheric convection before a substorm, which generates the westward electric field.

[43] The following increase of $h_m F2$ could be caused by the

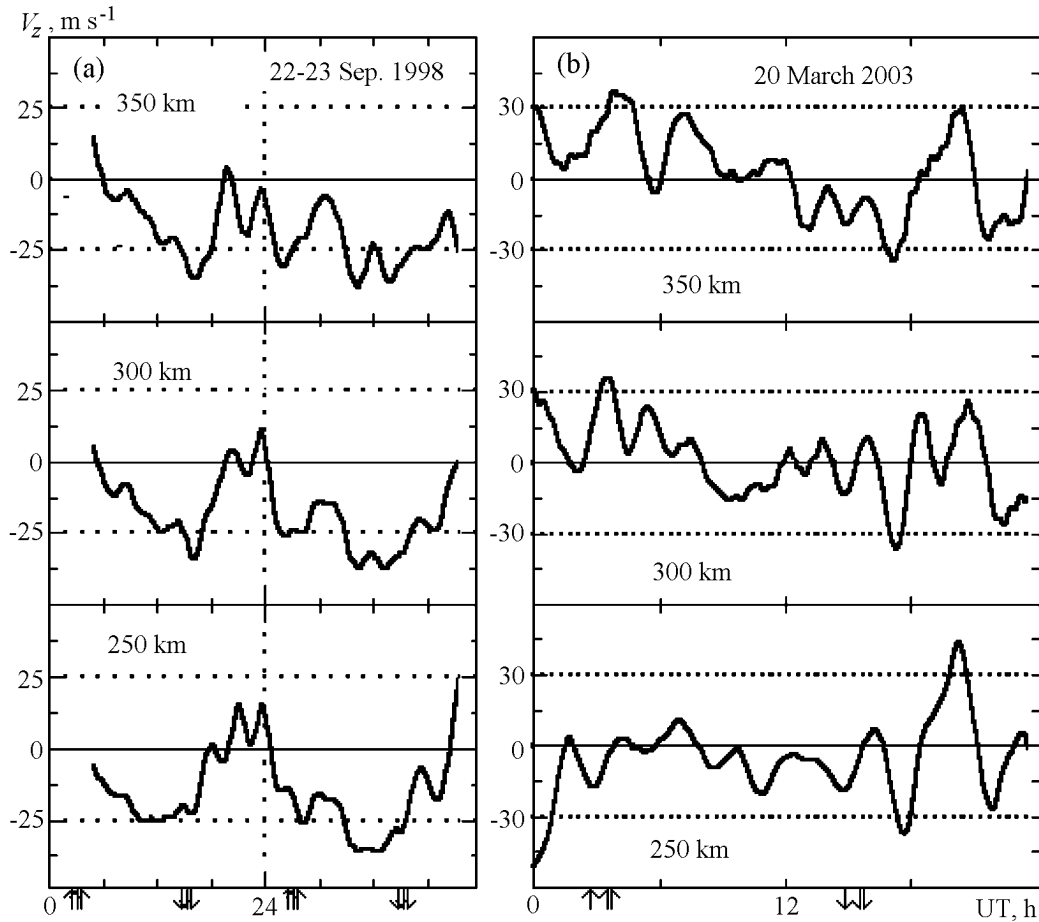


Figure 24. Variations of the vertical component of the plasma velocity V_z on the quiet days 22–23 September 1998 (left panel) and on the disturbed day 20 March 2003 (right panel).

regular equatorward turning of V_{nx} during the sunset, when $\Delta h_m F2 \approx 50$ km as on quiet days, and by the additional change in V_{nx} ($\Delta V_{nx} \approx 25$ m s^{-1}), which occurred in the preceding hours and was one of the reasons of the initial positive phase (see above). This additional change in V_{nx} could explain the $F2$ -layer lifting by about 20 km more.

[44] Now we consider the mechanisms that can explain the remaining increase of $h_m F2$ by about 130 km. One of these mechanisms could be the eastward electric field. If we assume that the registered uplifting of the $F2$ layer by 90 km during 15 min was caused by this electric field effects, we obtain $E_y \approx 15$ mV m^{-1} . The cases of such rapid eastward-westward switching of the electric field related to changes in the electrodynamic conditions during a magnetospheric substorm (gradients of conductivity, electric fields and currents at the edges of the westward auroral electrojet, nonstationary magnetospheric convection, etc.) were discussed, e.g., by Reddy and Nishida [1992]. One of the reasons of nonstationary magnetospheric convection could be the abrupt change of the solar wind parameters: the speed V_{sw} , IMF B_z component, the dynamic pressure p_{sw} around 1800 UT (see Figure 21).

[45] The second mechanism could be related to TAD,

which results in an increase in the $h_m F2$ after switching off of the previously acting westward electric field. TAD was able to provide the remaining 40-km lifting of the $F2$ layer. Such examples of a successive action of the electric field and TAD on the ionosphere were described, for example, by Reddy and Nishida [1992] and Pröls [1993b]. However, TAD effects should have been related to the earlier substorms (see Figure 21) with smaller intensity ($AE = 600 - 900$ nT). Nevertheless, the TAD effects were found out. They were observed as a delay of the velocity V_z disturbance that propagated from top to bottom (see Figure 24b). The delay was 80 min in altitude range of 400–200 km. This corresponded to a velocity of about 40 m s^{-1} , which is typical of the vertical component of IGW velocity. Besides, the V_z disturbance amplitude increased up to an altitude of 350 km and then began to decrease. Such features of the wave energy dissipation with an increase of height are also typical of IGWs. From this we can conclude that an increase of $h_m F2$ by about 130 km could result from the superposition of the effects of two sources: the eastward electric field, which is related to the intense substorm that occurred at 1800 UT ($AE = 1500$ nT), and TAD generated by the earlier substorm, e.g., after 1600 UT ($AE = 600 - 900$ nT).

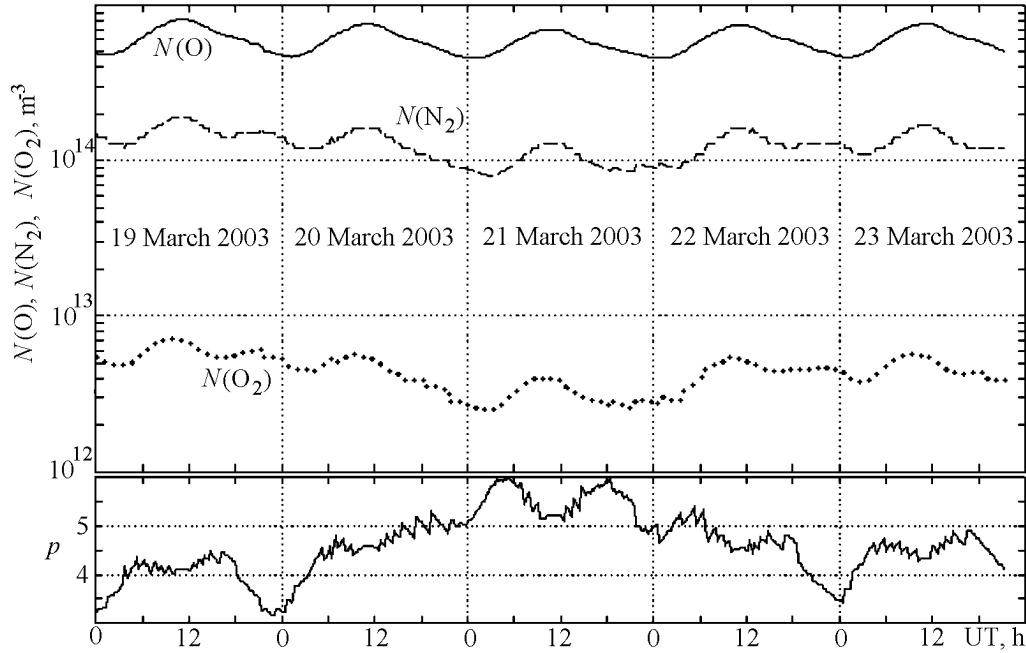


Figure 25. Time variations of concentration of the main neutral components and parameter p at the height of 300 km on 19–23 March 2003 from the NRLMSISE-00 model data.

[46] Thus an unusual behavior of $h_m F2$ during the sunset on 20 March can be explained in the following way. The 50-km decrease and the subsequent 90-km rapid increase in $h_m F2$ (within the total approximately 200-km increase) were probably caused by the nonstationary electric field, with the zonal component changing its direction from westward to eastward ($E_y = -10$ and $+15$ mV m $^{-1}$), which penetrated to midlatitudes. It should be mentioned that the $h_m F2$ variations correlated with the V_z changes from $+10$ to -35 m s $^{-1}$ and, later on, to $+20$ m s $^{-1}$ at an altitude of 300 km (see Figures 22c and 24b) in the time interval approximately 1700–1900 UT with a delay of about 20 min, which is typical for the effects caused by electric field disturbances in the ionosphere [Foster and Rich, 1998; Foster et al., 1998]. These disturbances were probably related to the intense substorm that occurred at 1800 UT (see Figure 21) when at auroral latitudes the electric field strength could reach $\sim 70 - 100$ m V m $^{-1}$ at the values of index $AE = 1000 - 1500$ nT [Krinberg and Tashchilin, 1984; Serebryakov, 1982]. Penetrating to midlatitudes, such a field could reach the calculated value $|E_y| \approx (10 - 15)$ mV m $^{-1}$ and destabilize the behavior of the ionospheric $F2$ layer. Besides, TAD, which could be caused by a less intensive substorm occurred after 1600 UT, also could contribute to an additional increase in $h_m F2$ by about 40 km.

[47] At the ionospheric storm phase reversal, the $N_m F2$ decrease approximately by a factor of 2 (whereas on the quiet day such decrease is by about 20%) became a beginning of a deep negative disturbance. The estimates showed [Grigorenko et al., 2005b, 2005d] that the decrease in $N_m F2$ could be caused by the increase in the downward plasma drift velocity V_z (see Figure 24b) and the change in the velocity W

by -25 m s $^{-1}$ near $F2$ -layer peak against a background, of $\beta(O^+)$ loss coefficient increase by a factor of almost 5 at a decrease in $h_m F2$ from 280 to 230 km (see Figure 22c). The further development in the depression in N_e (by a factor of 4–5 in the morning on 21 March), could be related to the change of neutral composition and increase in the $N(N_2)$ and $N(O_2)$ concentrations that should be maximum in the dawn sector. However, the NRLMSISE-00 model data did not confirm this assumption: $N(N_2)$ and $N(O_2)$ concentrations about noon on 21 March, on the contrary, decreased by a factor of 1.7 and p parameter increased by a factor of nearly 1.3 as compared to a quiet day on 19 March (Figure 25). Possibly, model requires the correction of the values of $N(N_2)$ and $N(O_2)$ as it was shown, e.g., by Pavlov et al. [2004]. Besides, one more mechanism (vibrational excitation of N_2 and O_2 molecules [Buonsanto, 1999; Pavlov, 1998; Pavlov et al., 1999; Richards et al., 1994]) could begin to operate at the sunrise when plasma rapidly warmed up (T_e increased to 2000–3500 K) against a background of low N_e values. This mechanism becomes substantial at $T_e \geq 2000$ K [Banks, 1969; Brunelly and Namgaladze, 1988; Pavlov et al., 1999; Shunk and Nagy, 1978]. The contribution of excited N_2 and O_2 molecules also accelerates the loss of O^+ ions.

[48] The considered minor magnetic storm did not cause considerable thermospheric disturbances. The daytime neutral temperature T_n as indicated calculations based on the radar data and NRLMSISE-00 model increased by approximately 50 and 100 K during the positive and negative ionospheric storm phases, respectively, as compared to quiet days on 19 and 23 March and the height of the thermopause where the atmosphere becomes isothermal was about 300 km (Figure 26). We established that the daytime T_n values obtained

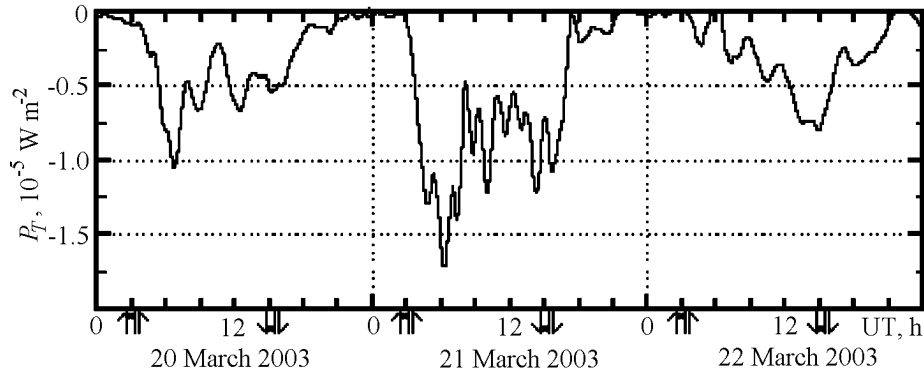


Figure 28. Time variations of the heat flux density P_T transported by electrons from the plasmasphere to the ionosphere at a height of 445 km during 20–22 March 2003.

5. Discussion

[50] The considered features of three magnetic storms and of the processes in the ionosphere over Kharkov that accompanied these storms make it possible to formulate the principal regularities in development of these processes. Conventionally the presented ionospheric storms may be split into two groups.

[51] The ionospheric storms accompanying the severe magnetic storms ($Kp \geq 8$) form the first group. These magnetic storms occurred on 25 September 1998 and 29–30 May 2003. They had long-lasting (6–9 hours) periods of high geomagnetic activity ($Kp \geq 8$), the active period of the main phase of the storms developed quickly with the maximum values $|Dst/dt| = 35 - 65 \text{ nT h}^{-1}$ and fell on the time interval when the Kharkov radar was in the midnight-predawn sectors. The ionospheric storms accompanying these magnetic storms are characterized by the considerable disturbances: the decrease in electron density by a factor of up to 3–4, increase in the height of the electron density peak $h_m F2$ by 100–160 km, nighttime heating of the plasma up to 2400–3200 K, increase in the neutral temperature by 200–350 K, increase in the thermopause height not less than to 400 km, infringement of the processes controlling thermal balance of the ionosphere and plasmasphere during a storm, and depletion by more than an order of magnitude of the relative density of hydrogen ions $N(\text{H}^+)/N_e$ during the storm main phase with its following increase during the recovery phase. One of the reasons of these disturbances could be the shift to midlatitudes of the main ionospheric trough, light ion trough, and hot zone to the geomagnetic shells L located deep within the inner plasmasphere. The nonstationary disturbances of magnetospheric electric fields accompanying the intensification of the auroral electrojets during a substorm on the background of a storm and also energetic particle precipitations from the magnetosphere could lead to a penetration of the magnetospheric electric fields into middle latitudes and destabilize the state of the ionosphere.

[52] The second group includes the ionospheric storm, which accompanied the minor magnetic storm on 20–21 March 2003 ($Kp \approx 5$). The magnetic storm began in

the morning (0445 UT), the main phase developed slowly ($|Dst/dt| \approx 5 \text{ nT h}^{-1}$) and reached minimum value of index $Dst = -57 \text{ nT}$ at 2000 UT. The ionospheric storm had a two-phase character and began with a positive phase. The prominent feature of this storm was that its negative phase occurring on the background of weak geomagnetic activity was accompanied by very strong ionospheric disturbances with a depletion in $N_m F2$ by a factor of up to 5, electron temperature increase up to 2400–3500 K at heights of 300–500 km, and uplifting in the $F2$ layer by more than 100 km during the night on 20–21 March and around sunrise. The reversal of the storm phase occurred during less than a hour in the dusk period was, apparently, caused by a superposition of the effects of two destabilizing factors generated by magnetospheric substorms: the pulse of the electric field in the ionosphere over Kharkov (with the E_y component changing the direction from the westward to the eastward and having the values of -10 and $+15 \text{ mV m}^{-1}$) and passage of TAD.

6. Conclusions

[53] The results of the studies of disturbances in the mid-latitude ionosphere over Kharkov during three geomagnetic storms distinguished by their intensity and occurred under moderate level of solar activity are presented.

[54] The obtained data showed that intense geomagnetic disturbances (on 25 September 1998 and 29–30 May 2003, $Kp \approx 8$) could be accompanied by phenomena rare for middle latitudes and related to the equatorward shift of the main ionospheric trough, light ion trough, and hot zone to the geomagnetic L shells located within the inner plasmasphere. The disturbances could lead to considerable changes in the structure of the ionospheric F region and thermal and dynamical regimes of the charged and neutral components of the Earth's upper atmosphere.

[55] The results of observations and modeling of the dynamical processes in the ionosphere showed that a geomagnetic storm of even a modest intensity (on 20–21 March 2003, $Kp \approx 5$) is capable of causing at middle latitudes

a strong negative ionospheric storm accompanied by considerable variations in ionospheric parameters. The reversal of the storm phases can be caused by a superposition of two destabilizing factors: electric field pulse and traveling atmospheric disturbance, both factors being generated by magnetospheric substorms.

[56] The obtained results are used in a study and modeling of disturbed ionosphere (including the processes accompanying the storm phases reversal) in the central Europe region.

[57] **Acknowledgments.** The authors are grateful to S. V. Chernyaev, Yu. V. Chernyak, L. Ya. Emel'yanov, and I. B. Sklyarov for the conduction of measurements at the IS radar and also to S. A. Pazura for performing computer simulations. The authors would also like to thank L. P. Goncharenko for her assistance and valuable comments during revision of the paper.

References

- Afraimovich, E. L., E. A. Kosogorov, L. A. Leonovich, and O. M. Pirog (2002), Global picture of large-scale ionospheric disturbances during the magnetic storm on 25 September 1998, *Geomagn. Aeron.* (in Russian), *42*(4), 491.
- Akimov, L. A., Ye. I. Grigorenko, V. I. Taran, O. F. Tyrnov, and L. F. Chernogor (2002), Coordinated radiophysical and optical studies of the dynamical processes in the atmosphere and space environment caused by the solar eclipse on 11 August 1999, *Progress Modern Radioelectr.* (in Russian), *2*, 25.
- Bailey, G. J., R. J. Moffett, and J. A. Murphy (1979), Calculated daily variations of O^+ and H^+ at mid-latitudes. II. Sunspot maximum results, *J. Atmos. Terr. Phys.*, *41*, 471, doi:10.1016/0021-9169(79)90038-2.
- Banks, P. M. (1966), Charged particle temperatures and electron thermal conductivity in the upper atmosphere, *Ann. Geophys.*, *22*, 577.
- Brunelly, B. E., and A. A. Namgaladze (1988), *Physics of the Ionosphere* (in Russian), Nauka, Moscow.
- Buonsanto, M. J. (1995a), Millstone Hill incoherent scatter F region observations during the disturbances of June 1991, *J. Geophys. Res.*, *100*, 5743, doi:10.1016/0021-9169(79)90038-2.
- Buonsanto, M. J. (1995b), A case study of the ionospheric storm dusk effects, *J. Geophys. Res.*, *100*, 23,857, doi:10.1029/95JA02697.
- Buonsanto, M. J. (1999), Ionospheric storms: A review, *Space Sci. Rev.*, *88*, 563, doi:10.1023/A:1005107532631.
- Buonsanto, M. J., S. A. Gonzalez, X. Pi, J. M. Ruohoniemi, M. P. Sulzer, W. E. Swartz, J. P. Thayer, and D. N. Yuan (1999), Radar chain study of the May, 1995 storm, *J. Atmos. Sol. Terr. Phys.*, *61*, 233, doi:10.1016/S1364-6826(98)00134-5.
- Chernogor, L. F., Ye. I. Grigorenko, V. I. Taran, and O. F. Tyrnov (2002a), Dynamic processes in the near-Earth plasma during the September 25, 1998 magnetic storm from Kharkov incoherent scatter radar data, in *Proc. XXVII General Assembly of the International Union of Radio Science, Maastricht, Netherlands*, p. 99, URSI, Maastricht, Netherlands.
- Chernogor, L. F., Ye. I. Grigorenko, V. I. Taran, and O. F. Tyrnov (2002b), Ionosphere wave-like disturbances (WLD) following the September 23, 1998 solar flare from Kharkov incoherent scatter radar observations, in *Proc. XXVII General Assembly of the International Union of Radio Science, Maastricht, Netherlands*, p. 99, URSI, Maastricht, Netherlands.
- Dalgarno, A., and T. C. Degges (1968), Electron cooling in the upper atmosphere, *Planet. Space Sci.*, *16*, 125, doi:10.1016/0032-0633(68)90049-4.
- Danilov, A. D., and L. D. Morozova (1985), Ionospheric storms in the F_2 region. Morphology and physics (a review), *Geomagn. Aeron.* (in Russian), *25*(5), 705.
- Danilov, A. D., L. D. Morozova, and E. G. Mirmovich (1985), A possible nature of the positive phase of ionospheric storms, *Geomagn. Aeron.* (in Russian), *25*(5), 768.
- Emel'yanov, L. Ya. (1999), Measurements of the drift velocity of the ionospheric plasma with the help of an incoherent scatter radar, *Proc. Kharkov Polytech. Univ.* (in Russian), *7*(3), 343.
- Evans, J. V. (1969), Theory and practice of ionosphere study by Thomson scatter radar, *Proc. IEEE*, *57*(4), 496.
- Farley, D. T. (1969), Faraday rotation measurements using incoherent scatter, *Radio Sci.*, *4*, 143.
- Foster, J. C., and F. J. Rich (1998), Prompt midlatitude electric field effects during severe geomagnetic storms, *J. Geophys. Res.*, *103*, 26,367, doi:10.1029/97JA03057.
- Foster, J. C., S. Cummer, and U. S. Inan (1998), Midlatitude particle and electric field effects at the onset of the November 1993 geomagnetic storm, *J. Geophys. Res.*, *103*, 26,359, doi:10.1029/98JA00018.
- German, J. R., and R. A. Goldberg (1981), *Sun, Weather and Climate* (in Russian), 320 pp., Gidrometeoizdat, St. Petersburg.
- Ginzburg, V. L. (1967), *Propagation of Electromagnetic Waves in Plasma* (in Russian), 684 pp., Nauka, Moscow.
- Gonzales, C. A., M. C. Kelley, R. A. Behnke, J. F. Vickrey, R. Wand, and J. Holt (1983), On the latitudinal variations of the ionospheric electric field during magnetospheric disturbances, *J. Geophys. Res.*, *88*, 9135.
- Grigorenko, Ye. I. (1979), Studies of the ionosphere based on the Faraday effect observations during incoherent scatter of radiowaves, *Ionos. Stud.* (in Russian), *27*, 60.
- Grigorenko, Ye. I., S. V. Lazorenko, V. I. Taran, and L. F. Chernogor (2003a), Ionospheric wave disturbances accompanied by the solar flare and the strongest magnetic storm of September 25, 1998, *Geomagn. Aeron.* (in Russian), *43*(6), 718.
- Grigorenko, Ye. I., V. N. Lysenko, V. I. Taran, and L. F. Chernogor (2003b), Results of radiophysical studies of the processes in the ionosphere accompanying the very strong magnetic storm on 25 September 1998, *Progress Mod. Radioelectr.* (in Russian), *9*, 57.
- Grigorenko, Ye. I., L. Ya. Emel'yanov, S. A. Pazura, V. A. Pulyaev, V. I. Taran, and L. F. Chernogor (2005a), Disturbances in the ionospheric plasma during the severe magnetic storm on 29–31 May 2003: The results of observations with the Kharkov incoherent scatter radar, *Progress Mod. Radioelectr.* (in Russian), *4*, 21.
- Grigorenko, Ye. I., V. N. Lysenko, V. I. Taran, and L. F. Chernogor (2005b), Specific features of the ionospheric storm of March 20–23, 2003, *Geomagn. Aeron.* (in Russian), *45*(6), 745.
- Grigorenko, Ye. I., S. A. Pazura, V. I. Taran, L. F. Chernogor, and S. V. Chernyaev (2005c), Dynamic processes in the ionosphere during the severe magnetic storm of May 30–31, 2003, *Geomagn. Aeron.* (in Russian), *45*(6), 758.
- Grigorenko, Ye. I., V. I. Taran, L. F. Chernogor, and S. V. Chernyaev (2005d), Anomalous ionospheric storm on 21 March 2003: The results of observations with the Kharkov incoherent scatter radar, *Progress Mod. Radioelectr.* (in Russian), *4*, 3.
- Holt, J. M., D. A. Rhoda, D. Tetenbaum, and A. P. van Eyken (1992), Optimal analysis of incoherent scatter radar data, *Radio Sci.*, *27*, 435.
- Krinberg, I. A., and A. V. Tashchilin (1984), *Ionosphere and Plasmasphere* (in Russian), Nauka, Moscow.
- Lysenko, V. N. (1999a), Peculiarities of the correlation processing of IS signal at ionospheric sounding in the meter range by radio pulses 800 μ s duration, *Proc. Kharkov Polytech. Univ.* (in Russian), *31*, 90.
- Lysenko, V. N. (1999b), Statistical errors of measurements of the electron and ion temperatures, *Proc. Kharkov Polytech. Univ.* (in Russian), *7*(3), 355.

- Lysenko, V. N. (2001), Measurements of the vertical component of the plasma drift velocity and kinetic temperatures in the ionosphere, *Geomagn. Aeron.* (in Russian), *41*(3), 365.
- Mikhailov, A. V., and M. Förster (1999), Some F2-layer effects during the January 06–11, 1997 CEDAR storm period as observed with the Millstone Hill Incoherent Scatter Facility, *J. Atmos. Sol. Terr. Phys.*, *61*, 249, doi:10.1016/S1364-6826(98)00129-1.
- Mikhailov, A. V., and J. C. Foster (1997), Daytime thermosphere above Millstone Hill during severe geomagnetic storms, *J. Geophys. Res.*, *102*, 17,275, doi:10.1029/97JA00879.
- Mikhailov, A. V., and K. Schlegel (1997), Self-consistent modelling of the daytime electron density profile in the ionospheric F region, *Ann. Geophys.*, *15*, 314, doi:10.1007/s005850050446.
- Mishin, E., J. C. Foster, F. J. Rich, and V. I. Taran (2001), Prompt ionospheric response to short period solar wind variations during the magnetic cloud event Sep. 25, 1998, *Eos Trans. AGU, Spring Meet. Suppl.*, *82*(20), S291.
- Mishin, E. V., J. C. Foster, A. P. Potekhin, F. J. Rich, K. Schlegel, K. Yumoto, V. I. Taran, M. J. Ruohoniemi, and R. Friedel (2002), Global ULF disturbances during a stormtime substorm on 25 September 1998, *J. Geophys. Res.*, *107*(A12), 1486, doi:10.1029/2002JA009302.
- Naghmoosh, A. A., and J. A. Murphy (1983), A comparative study of H⁺ and He⁺ at sunspot minimum and sunspot maximum, *J. Atmos. Sol. Terr. Phys.*, *45*(10), 673, doi:10.1016/S0021-9169(83)80026-9.
- Pavlov, A. V. (1998), The role of vibrationally excited oxygen and nitrogen in the ionosphere during the undisturbed and geomagnetic storm period of 6–12 April 1990, *Ann. Geophys.*, *16*, 589, doi:10.1007/s00585-998-0589-5.
- Pavlov, A. V., and M. J. Buonsanto (1996), Using steady-state vibrational temperatures to model effects of N₂^{*} on calculations of electron densities, *J. Geophys. Res.*, *101*, 26,941, doi:10.1029/96JA02734.
- Pavlov, A. V., M. J. Buonsanto, A. C. Schlesier, and P. J. Richards (1999), Comparison of models and data at Millstone Hill during the 5–11 June 1991 storm, *J. Atmos. Sol. Terr. Phys.*, *61*, 263, doi:10.1016/S1364-6826(98)00135-7.
- Pavlov, A. V., N. M. Pavlova, and S. F. Makarenko (2004), Study of thermal balance of ionosphere and thermosphere at midlatitudes from the Millstone Hill radar data during January 14–17, 1986, *Geomagn. Aeron.* (in Russian), *44*(2), 204.
- Picone, J. M., A. E. Hedin, D. P. Drob, and A. C. Aikin (2002), NRLMSISE-00 empirical model of the atmosphere: Statistical comparisons and scientific issues, *J. Geophys. Res.*, *107*(A12), 1468, doi:10.1029/2002JA009430.
- Prölss, G. W. (1993a), On explaining the local time variation of ionospheric storm effects, *Ann. Geophys.*, *11*, 1.
- Prölss, G. W. (1993b), Common origin of positive ionospheric storms at middle latitudes and the geomagnetic activity effect at low latitudes, *J. Geophys. Res.*, *98*, 5981.
- Prölss, G. W. (1995), Ionospheric F-region storms, in *Handbook of Atmospheric Electrodynamics*, vol. 2, edited by H. Volland, p. 195, CRC Press, Boca Raton, Fla.
- Pulyaev, V. A. (1999), Processing and presentation of the incoherent scatter data, *Proc. Kharkov Polytech. Univ.* (in Russian), *31*, 84.
- Reddy, C. A., and A. Nishida (1992), Magnetospheric substorms and nighttime height changes of the F2 region at middle and low latitudes, *J. Geophys. Res.*, *97*, 3039.
- Richards, P. G., D. G. Torr, M. J. Buonsanto, and D. P. Sipler (1994), Ionospheric effects of the March 1990 magnetic storm: Comparison of theory and measurement, *J. Geophys. Res.*, *99*, 23,359.
- Saenko, Yu. S., V. V. Klimenko, and A. A. Namgaladze (1982), Studies of the process of filling in and emptying of plasma tubes taking into account the ion inertia, *Geomagn. Aeron.* (in Russian), *22*(6), 948.
- Salah, J. E., and J. V. Evans (1973), Measurements of thermospheric temperature by incoherent scatter radar, *Space Res.*, *13*, 267.
- Salah, J. E., J. V. Evans, D. Alcaydè, and P. Bauer (1976), Comparison of exospheric temperatures at Millstone Hill and St-Santin, *Ann. Geophys.*, *32*(3), 257.
- Schlesier, A. C., and M. J. Buonsanto (1999), The Millstone Hill ionospheric model and its application to the May 26–27, 1990, ionospheric storm, *J. Geophys. Res.*, *104*, 22,453, doi:10.1029/1999JA900250.
- Serebryakov, B. E. (1982), Studies of the processes in the thermosphere during magnetic disturbances, *Geomagn. Aeron.* (in Russian), *22*(5), 776.
- Shunk, R. W., and A. F. Nagy (1978), Electron temperature in the F region of the ionosphere: theory and observations, *Rev. Geophys. Space Phys.*, *16*(3), 355.
- Taran, V. I. (1979), Incoherent scatter of radio waves at thermal fluctuations of the electron density, *Ionos. Stud.* (in Russian), *27*, 19.
- Taran, V. I. (2001), Studies of the ionosphere in natural and disturbed conditions by the incoherent scatter method, *Geomagn. Aeron.* (in Russian), *41*(5), 659.
- Taran, V. I., Ye. I. Grigorenko, V. N. Lysenko, and V. A. Pulyaev (1999), Ionospheric effects of magnetic storms as observed at Kharkov incoherent scatter radar, *Proc. Kharkov Polytech. Univ.* (in Russian), *7*(3), 381.
- Vladimirsky, B. M., K. N. Cidyakin, and N. A. Temur'yantz (1995), *Cosmos and Biological Rhythms*, 156 pp., Eupatoria City Typography, Sympheropol, Ukraine.
- Waldteufel, P. (1971), Combined incoherent scatter F1 region observations, *J. Geophys. Res.*, *76*, 6995.

L. F. Chernogor, Kharkov V. Karazin National University, Kharkov, Ukraine. (Leonid.F.Chernogor@univer.kharkov.ua)

Ye. I. Grigorenko, V. N. Lysenko, and V. I. Taran, Institute of the Ionosphere, National Academy of Sciences of Ukraine, Ministry of Education and Science of Ukraine, Kharkov, Ukraine. (iion@kpi.kharkov.ua)